DESIGN OF BIOAEROSOL SAMPLING INLETS

A Thesis

by

ROHIT RAVINDRA NENE

Submitted to the Office of Graduate Studies of
Texas A&M University
in partial fulfillment of the requirements for the degree of

MASTER OF SCIENCE

May 2006

Major Subject: Mechanical Engineering

DESIGN OF BIOAEROSOL SAMPLING INLETS

A Thesis

by

ROHIT RAVINDRA NENE

Submitted to the Office of Graduate Studies of
Texas A&M University
in partial fulfillment of the requirements for the degree of

MASTER OF SCIENCE

Approved by:

Chair of Committee,	Andrew R. McFarland
Committee Members,	John S. Haglund
	Yassin A. Hassan
Head of Department,	Dennis L. O'Neal

May 2006

Major Subject: Mechanical Engineering

ABSTRACT

Design of Bioaerosol Sampling Inlets. (May 2006)

Rohit Ravindra Nene, B.Tech., Indian Institute of Technology, Madras, India

Chair of Advisory Committee: Dr. Andrew R. McFarland

An experimental investigation involving the design, fabrication, and testing of an ambient sampling inlet and two additional Stokes-scaled inlets is presented here. Testing of each inlet was conducted at wind speeds of 2, 8, and 24 km/h (0.55, 2.22, and 6.67 m/s), and characterized for particle sizes between 5 and 20 µm AD. The base-line ambient sampling inlet, which operates at 100 L/min, was developed to interface with a Circumferential Slot Virtual Impactor aerosol concentrator. The inlet displays wind-speed independent characteristics with a penetration above 90% for a nominal particle size of 10 µm AD for all wind speeds. Particles up to 11.5 µm AD are sampled through this inlet with a penetration above 80% at all wind speeds. In an effort to test the validity of Stokes scaling to assist in the design of inlets, two additional inlets were designed to accommodate design flow rates of 400 L/min and 800 L/min, with the 100 L/min unit as the base inlet. Scaling was achieved by applying a Stokes scaling factor to selective parameters, such as inlet aspiration gap, annular gap, window height, and the rise which is the vertical distance extending from the lower flange to the base of the window. The scaled inlets display wind independent penetration characteristics close to 95% for a nominal particle size of 10 µm AD. The scaled inlets also have the ability to sample particles up to a size of 13 µm AD with a penetration in excess of 80% at all wind speeds.

Observations from the plots of penetration against the Stokes number based on the free stream velocity suggest that it is insufficient to use only Stokes-scaling for inlet design. A modified velocity ratio defined for omnidirectional inlets was incorporated into a summary of results obtained for all combinations of BSI units and wind speeds. Also, a correlation equation based on the Stokes number and a modified velocity ratio was developed as a model for predicting performance among the BSI family of inlets. This correlation used in unison with Stokes-scaling provides promise for predicting performance and improving the overall design process of inlets.

DEDICATION

To my parents for their unwavering love, support, and encouragement.

ACKNOWLEDGEMENTS

Funding for this project was provided by The Research Development and Engineering Command (RDECOM) of the U.S. Army under Contract Number DAAD13-03-C-0050 issued to the Texas Engineering Experiment Station (Project Numbers 32579-60240 and 32579-6024E). Dr. Jerold R. Bottiger and Mr. Samuel P. Leppert are the Contract Technical Managers for the U.S. Army. The technical and financial support provided by the Army is greatly appreciated.

The successful completion of this study is also attributed to the contributions, endless support and guidance from the following individuals with whom I have interacted throughout this academic endeavor:

- Dr. Andrew McFarland, my advisor and committee chair, for his continued guidance, motivation, and words of wisdom.
- Dr. John Haglund, my committee member and colleague, for his technical astuteness and faith in my abilities.
- Dr. Yassin Hassan, my committee member, for his guidance and support of my academic interests.
- Mr. Carlos Ortiz, my colleague and friend, for his endless supply of technical advice, support and motivation during our daily encounters at USB.
- Mr. Mark Dunn and Ms. Janie Dunn of Spiral Fittings Inc. of South Carolina, for their skill, efficiency, and amiability in delivering quality products.
- Mr. James Dworaczyk of Machine Works (Bryan, TX) for his skill and suggestions provided on a gamut of machined parts.

- My colleagues, peers, and friends at the Aerosol Technology Laboratory at Texas A&M University for their support and friendship.

TABLE OF CONTENTS

Page

LIST OF TABLES

LIST OF FIGURES

FIGURE Page

FIGURE Page

INTRODUCTION

Background

Biological weaponry may be thought to be in its infancy, but it has been used for centuries as a modality of war. It is only in more recent times that domestic acts of bioterrorism such as the anthrax (*Bacillus anthracis*) attacks in 2001 and the ricin incidents of 2003 in Washington D.C. have caused a growing concern towards the issue of national security of the United States. Improving response capabilities, both in the civilian and military sectors, through timely detection and identification of biological warfare agents, is seen as an imminent course of action.

Effective and timely response to a situation depends on the type of biological agent detection system. Near-real-time point detection technologies contain sensors that must be in the presence of the aerosol plume or have the suspect biological agent introduced to them for sensing. Point detection systems traditionally have the following components: sampler, trigger or cue, and an identifier.

In an effort to develop a near-real-time biological point detection system, the U.S. Military has effected several programs including the Joint Biological Point Detection System (JBPDS), to replace previously existing systems such as the Biological Integrated Detection System (BIDS) and the Interim Biological Agent Detector (IBAD). These systems have been deployed by the U.S. Army and the U.S. Navy (Wolf and Hohe, 2000). In the presently deployed configuration, the JBPDS samples at 780 L/min. The inlet sampler currently used for this system is shown in Figure 1. In support of the U.S.

This thesis follows the style and format of *Aerosol Science and Technology*.

Military bioaerosol detection effort, the Aerosol Technology Laboratory (ATL) of the Texas Engineering Experiment Station conducts research and development under contract from the U.S. Army Research and Development Engineering Command (RDECOM). Work is currently underway at ATL to upgrade the sampling system capabilities of the JBPDS from an existing sampling flow rate of about 800 L/min to 1250 L/min, which entails development of a new inlet.

Aerosol Sampling

The sampling of aerosol particles ideally involves obtaining an accurate representation of the size distribution, concentration and composition that is present in the free stream or ambient environment, with the sample characteristics independent of sampling conditions for all particles of interest. The sampling of aerosols can be broadly classified into four categories; a) ambient sampling, which is the sampling from the free atmosphere; b) source sampling, which involves sampling from ducts, stacks, pipes, and moving fluid streams; c) occupied environment sampling; and d) sampling from a moving platform such as an aircraft, land-based vehicle, or ship. In this thesis, the focus is on ambient sampling systems. It may be necessary to point out that the motivation for aerosol inlet design studies extends far beyond the problems related to biological agent detection. Ambient monitoring of environmental pollutants, perimeter monitoring of industrial and nuclear facilities, and global monitoring of radionuclides are a few other applications where inlet design is critical.

The increasing significance of ambient sampling has given rise to the establishment of various standards on permissible values of aerosol concentration. In the

last few decades, many changes have been effected in the characterization of atmospheric particulate matter, which until 1972 was primarily accomplished through the use of samples acquired with high volume ("Hi-Vol") devices. These samplers measure total suspended particulate (TSP) while drawing in air at a flow rate of 1.41 m^3/min (50 CFM). This approach was considered inadequate because the collected sample contained particles with sizes larger than those that would penetrate into the thoracic region of the human lung system. The TSP standard was health-based, and the non-thoracic fraction of the aerosol was not considered to be an important factor in impacting human health (Wedding, 1982). Also, the collection capability of samplers was found to be a strong function of particle size, wind speed, and sampler orientation. These shortcomings prompted the U.S. Environmental Protection Agency (EPA) to examine fractionating the ambient aerosol sample prior to collection. Initially, it was recommended that the fractionation curve should exhibit a cutpoint of 15 μm AD, however that was subsequently changed to 10 μm AD. The cutpoint (D_{50}) is the aerodynamic diameter (AD) that is associated with 50% inlet aerosol penetration. The aerodynamic diameter (AD) of a particle is defined as the diameter of a spherical particle with a density of 1000 kg/m^3 (the density of a water droplet) that has the same settling velocity as the particle of interest (Hinds, 1999). Particulate matter that penetrates through a fractionator with a cutpoint of 10 μm AD is called PM-10. Because of the concern over the health effects of fine particles in air, the EPA adopted new standards for sampling fine particles, PM-2.5 (Federal Reference Method, PM-2.5). These standards are designed to provide the basis for controlling particles smaller than 2.5 μm in aerodynamic diameter, which pose a

significant risk to human health because of their ability to penetrate and deposit in the bronchial and alveolar regions of the respiratory duct.

In addition to physical considerations, there are biological considerations inherent to bioaerosol sampling that need to be addressed to present a holistic approach to the research at hand. For example, biological sampling may require aseptic handling to prevent contamination and special attention to the viability of the organisms during the process of sampling and analysis (Hinds, 1999). This study deals with the ambient sampling of bioaerosols, and focuses on the physical aspect of bioaerosol sampling without considering the details of the biological aspects of the aerosol particles.

Inlets for Aerosol Sampling

The detection of biological agents is carried out by extracting a sample of air from the contaminated environment and passing it to other sampling system components such as a concentrator, collector, lysing device, etc. before presenting the sample to a detector or identifier.

Ambient bioaerosol sampling at high volumetric flow rates, is generally an essential part and the first step towards proper agent detection, with current field systems operating at sample flow rates of the order of 1000 L/min. The inlet of the bioaerosol sampling system, which aspirates the sample ambient atmosphere, ideally allows all particles of interest to enter and arrive at the detector or identifier without harming or altering the agent, yet excluding rain, snow, insects, plant matter, and other airborne debris. Generally, an inlet will include a fractionator, such as an impactor or cyclone, and a screen to strip the unwanted debris from the size distribution. An efficient inlet is

one in which particle losses due to impaction on external surfaces, turbulent deposition, and sedimentation are minimized (Liu and Pui, 1981). The performance of the inlet should also remain unaffected by changes in wind speed and direction. In this study the basic performance characteristics of the inlet will be investigated, independent of the presence of either a screen or fractionator. The rationale for this approach is that if an inlet sans screen or fractionator can aspirate and transmit bioaerosol particles in the size range of interest at a high level of penetration, then a screen and fractionator can customize the size distribution to fit the needs of the user.

Depending on the type of application, different basic inlet design styles may be considered. Unidirectional inlets such as shrouded probes are used predominantly in source sampling and mobile-platform applications, where the direction of the free stream is known. In the case of ambient sampling, the free stream direction is highly variable and a properly designed inlet should be able to sample independent of wind direction. A traditional omnidirectional inlet has a circumferential intake that allows particles to be aspirated regardless of the wind direction. The present study encompasses the design of a family of omnidirectional inlets.

THEORY

There exist several parameters that can serve as metrics to capture the performance of an inlet. The penetration of aerosol through an inlet is an extensively used parameter. For a particle size interval that is represented by an aerodynamic diameter of $D_{a,i}$ the aerosol penetration is

$$P_i = \frac{C_{e,i}}{C_{\infty,i}} \qquad [1]$$

where $C_{e,i}$ is the aerosol concentration at the exit plane of the inlet, and $C_{\infty,i}$ is the aerosol concentration in the free stream. Because the present study is concerned with inlets devoid of fractionators, other parameters such as inlet effectiveness and collection efficiency will not be considered.

As a general observation from fluid flow principles, particle aspiration from the ambient atmosphere into an inlet is governed by the streamlines which carry the particles. In sampling sources or sampling from moving platforms, the concept of isokinetic sampling can be used to determine if a representative sample of aerosol arrives at the inlet plane of a sampling nozzle. Sampling is isokinetic when the inlet axis of the sampler, e.g., a thin-walled tube or probe, is aligned parallel to the gas streamlines and the gas velocity at the probe entrance plane equals the free stream velocity approaching the inlet. However, due to the possibility of internal wall losses in the nozzle, the condition of isokineticity is no assurance that the penetration will be unity.

Anisokinetic sampling may occur if the probe axis is not aligned with the gas flow streamlines or if the velocity in the probe is not equal to that of the free stream. If the velocity at the nozzle entrance plane is higher than that of the free stream ($U_{in}/U_o>1$), the

sampling is referred to as being superisokinetic; and if the velocity at the probe entrance plane is lower than that of the free stream ($U_{in}/U_o<1$), the sampling is said to be subisokinetic. Here, U_{in} is the spatial mean air velocity at the inlet plane of the nozzle and U_o is the free stream velocity.

As discussed earlier, ambient sampling introduces the challenge of sampling from an unknown direction, which is why omnidirectional inlets are usually suitable. Although isokinetic sampling and an associated velocity ratio exist for isoaxial sampling through a tube-like probe, it is proposed to extend this concept to the family of circumferential intake inlets. Because the airflow and particle behavior in an inlet are very complex, an analytical theory to relate penetration to parameters such as the velocity ratio is not possible. In this study, consideration will be given to experimentally examining the effect of such parameters upon aerosol penetration.

A simple dimensional analysis has been performed below using Buckingham's Π-theorem and establishing a set of dimensionless π-groups. The aerosol penetration through an inlet, P, is known to be functionally dependent on the following variables:

$$P = P\left(\tau, U_o, d_c, \rho, \mu, U^*\right) \qquad [2]$$

where

τ is the particle relaxation time;

U_o is the free stream velocity;

d_c is a characteristic dimension of the inlet;

ρ is the density of air;

μ is the dynamic viscosity of air; and

U^* is a reference velocity (a reflection of the flow rate, Q) inside the inlet.

These variables can be expressed in terms of their fundamental units of mass, M, length, L, and time, T.

$[\tau] = T$;

$[U_o] = LT^{-1}$;

$[d_c] = L$;

$[\rho] = ML^{-3}$;

$[\mu] = ML^{-1}T^{-1}$;

$[U^*] = LT^{-1}$.

According to Buckingham's Π-theorem, the number of dimensionless π-groups is given by the difference in the number of independent variables, m and the number of fundamental dimensions used to express the variables, n. Therefore, the number of π-groups is $(m - n)$, or $(6 - 3) = 3$ dimensionless π-groups.

$$\phi(\pi_1, \pi_2, \pi_3) = 0 \qquad [3]$$

If we choose the recurring variables to be U_i, d_c, and ρ, where U_i is one reference velocity – either U_o or U^* (the other reference velocity denoted as U_j), the dimensionless π-groups can be obtained as follows.

$$\pi_1 = U_i^{a_1} \cdot d_c^{b_1} \cdot \rho^{c_1} \cdot \tau \qquad [4]$$

$$M^0 L^0 T^0 = \left(LT^{-1}\right)^{a_1} \cdot (L)^{b_1} \cdot \left(ML^{-3}\right)^{c_1} \cdot T \qquad [5]$$

Solving for the coefficients we get $a_1 = 1$, $b_1 = -1$, and $c_1 = 0$.

$$\therefore \pi_1 = \frac{\tau \cdot U_i}{d_c} \qquad [6]$$

Similarly,

$$\pi_2 = U_i^{a_2} \cdot d_c^{b_2} \cdot \rho^{c_2} \cdot \mu \qquad [7]$$

$$M^0L^0T^0 = \left(LT^{-1}\right)^{a_2} \cdot \left(L\right)^{b_2} \cdot \left(ML^{-3}\right)^{c_2} \cdot ML^{-1}T^{-1} \quad [8]$$

Solving for the coefficients we get $a_2 = -1$, $b_2 = -1$, and $c_2 = -1$.

$$\therefore \pi_2 = \frac{U_i \cdot d_c \cdot \rho}{\mu} \quad [9]$$

Also,

$$\pi_3 = U_i^{a_3} \cdot d_c^{b_3} \cdot \rho^{c_3} \cdot U_j \quad [10]$$

$$M^0L^0T^0 = \left(LT^{-1}\right)^{a_3} \cdot \left(L\right)^{b_3} \cdot \left(ML^{-3}\right)^{c_3} \cdot LT^{-1} \quad [11]$$

Solving for the coefficients we get $a_3 = -1$, $b_3 = 0$, and $c_3 = 0$.

$$\therefore \pi_3 = \frac{U_i}{U_j} \quad [12]$$

The dimensionless parameters, π_1, π_2, and π_3, can be identified as the Stokes number, Reynolds number, and a velocity ratio, respectively.

$$P = P\left(Stk, \mathrm{Re}, \frac{U^*}{U_o}\right) \quad [13]$$

In the case of inlets, the Stokes number represents particle motion as warranted by the free stream wind speed, U_o. The Reynolds number can be used to describe the mechanics of internal flow within the inlet so the velocity in this case is U^*, a reference velocity associated with flow inside the inlet. The third π-group represents a ratio of the two reference velocities mentioned above; U^* and U_o. The ratio U^*/U_o is a velocity ratio which describes the interaction of the external flow field (free stream wind) and the internal flow field (sampling flow).

Fundamental theory on inertial impaction of aerosol particles suggests that the process is largely driven by the Stokes number rather than the Reynolds number (Hinds,

1999). The dominance of the Stokes number on particle motion indicates that the Reynolds number exists as a second order variable. If we extend the concept of inertial impaction to the particle behavior associated with inlets we can conclude that penetration may be represented as a function of the Stokes number and the velocity ratio.

$$\therefore P = P\left(Stk, \frac{U^*}{U_o} \right) \qquad [14]$$

Two reference velocities are required to completely describe the inlet dynamic model. One velocity is U_o, the velocity of the free stream; the other is U^*, which is defined as the volumetric flow rate of the inlet, Q, divided by a reference flow area in the inlet, A_{ref}. For the present study A_{ref} is the annular area between two concentric cylinders of the inlet. Also, the actual velocity in the gap depends on the external wind speed, so if the external wind speed is zero, the actual gap velocity reduces to Q/A_{ref}. The two reference velocities can be used to define a modified velocity ratio, U^*/U_o.

The employment of Stokes scaling is potentially an important tool to assist in the design of inlets used for sampling inertially-affected aerosol particles. The Stokes number is defined as the ratio of the stopping distance of a particle to a characteristic dimension of the system in the region where the stopping distance is being considered. In the case of flow perpendicular to a cylinder of diameter d_c the Stokes number is defined as

$$Stk = \frac{\tau \cdot U_{ref}}{d_c} \qquad [15]$$

where τ is the relaxation time and U_{ref} is the undisturbed air velocity. As the Stokes number approaches zero, particles track the streamlines perfectly. However, as the

Stokes number increases, particles resist changing their directions when there is curvature of the gas streamlines (Hinds 1999).

If the performance of a given inlet is known, it would be possible to infer the size or volumetric flow rate of a geometrically similar inlet if the Stokes number were solely responsible for characterizing particle penetration through the inlet. As an example, if the performance of an inlet (denoted with subscript "1") were known, then the performance of a second geometrically similar inlet (denoted with subscript "2") would be identical if the Stokes numbers of the two inlets were the same, i.e.

$$Stk_1 = Stk_2 \Rightarrow \left(\frac{\tau \cdot U_{ref}}{d_c} \right)_1 = \left(\frac{\tau \cdot U_{ref}}{d_c} \right)_2 \qquad [16]$$

If we choose to sample the same particle sizes with the two inlets, the relaxation times are the same for both inlets and can be cancelled on both sides. Assume that the reference velocity can be represented by the volumetric flow rate Q divided by a reference area, A_{ref}, in the zone where particle losses are taking place. In turn, assume that this area is proportional to the square of the characteristic dimension, i.e. to d_c^2. The above equation may be rewritten and subsequently rearranged to arrive at a scaling ratio.

$$\left(\frac{Q}{d_c^{\,3}} \right)_1 = \left(\frac{Q}{d_c^{\,3}} \right)_2 \qquad [17]$$

$$\frac{d_{c_2}}{d_{c_1}} = \sqrt[3]{\frac{Q_2}{Q_1}} \qquad [18]$$

Thus, if the operating volumetric flow rates of both inlets are known, the size of the desired inlet can be calculated. Alternatively, if the geometry of the desired inlet is scaled from a given inlet, the volumetric flow rate of the desired inlet may be determined, assuming the same performance holds.

If the performance of a given inlet is known in terms of its cutpoint, D_{50}, for a fixed volumetric flow rate, the cutpoint, D_{50} or the physical size of another inlet may also be determined from the Stokes scaling. The particle relaxation time, τ is proportional to the square of the particle diameter, D_p. Equating the Stokes number for two inlets assuming the volumetric flow rates to be equal gives

$$\left(\frac{D_{50}^{\ 2}}{d_c^{\ 3}}\right)_1 = \left(\frac{D_{50}^{\ 2}}{d_c^{\ 3}}\right)_2 \qquad [19]$$

$$\text{or, } \left(\frac{D_{50_2}}{D_{50_1}}\right)^2 = \left(\frac{d_{c_2}}{d_{c_1}}\right)^3 \qquad [20]$$

For example, if a particular cutpoint, D_{50} is desired, an inlet can be dimensionally scaled from a given inlet with a known cutpoint. Alternatively, if the size of an inlet is known (which is a geometric scaling from a given inlet) the cutpoint, D_{50} of that inlet can be determined.

LITERATURE REVIEW

Overview

Until a little over two decades ago, little attention had been given to examining the basic fluid and aerosol mechanics associated with the problem of collecting an unbiased sample of atmospheric particulate matter independent of the environmental conditions. However, several investigators had studied the performance of simple collector geometries in wind tunnels.

Davies (1968) modeled the sampling efficiency of cylindrical inlets with the tube axis oriented parallel to the wind velocity. Later he analyzed sampling in cross winds. Agarwal (1972) extended the analysis by solving the Navier-Stokes equation to observe the flow pattern of cylindrical inlets.

Wedding et al. (1977) studied the performance of the standard Hi-Vol sampler followed by a broader study conducted by McFarland et al. (1979). These efforts were in response to the need for a shift from a sampler that measures total suspended particulate (TSP) to one that sizes segregated samples, i.e., strips large unwanted particles from the distribution.

A dichotomous sampler is a low volume (1 m^3/hr) device designed to provide fine and coarse aerosol separation and collection for subsequent elemental and chemical analysis and to provide reasonably simple manual or automatic operation (Stevens et al., 1977). Inlets for use with dichotomous samplers were developed by McFarland at Texas A&M University (TAMU) based on earlier work by McFarland et al. (1978). These inlets typically exclude particles larger than 15 µm AD.

Commercial versions of the TAMU inlet were manufactured by Sierra Instruments and Beckman Instruments. Particles enter circumferentially and rise through a stilling chamber before making a U-turn and being pulled through a concentric outlet pipe. Wind tunnel tests conducted at TAMU indicate that particle collection is not severely affected by wind speeds of 2, 8, and 24 km/h (McFarland et al., 1978).

Liu and Pui (1981) later designed, constructed and tested an inlet for sampling particles less than 15 μm aerodynamic diameter at a flow rate of 16.7 L/min. The external geometry of the inlet was selected to allow entry of large particles into the inlet, while an impactor was used to remove the coarse particles that could not enter the thoracic region of the human lung tree. The inlet displayed characteristics independent of wind speed up to 9 km/h (2.5 m/s). Later studies showed there to be problems with both the fractionator and with inadvertent ingestion of precipitation. McFarland and Ortiz (1982, Sierra-Andersen 246B) designed an impactor for the inlet, and Tolocka et al. (2001) designed an all-weather roof for the device.

A large effort over the past few decades has been driven towards using various approaches to ambient aerosol sampling. A turning point in the design thinking occurred when the design rationale for an inhalable particulate matter (IPM) inlet was established. According to Wedding (1982), as it is not practical or necessary to achieve isokinetic sampling in the field, the inlet must only effectively transport to the fractionating device the particle sizes of interest with consistent or predictable losses independent of the wind speed, direction, turbulent intensity and scale, and environmental conditions such as debris, insects, etc..

The need to develop an inlet that conforms to the sampling standards stated above is critical. In addition to the development of an inlet for a specific application, a general design tool such as scaling should be implemented and validated in order to be able to take existing inlets and modify them to suit other applications.

Seo (2004) worked with various scaled versions of the modified Liu and Pui type inlets including a unit that was designed for a 780 L/min flow rate system, which is called the 780 L/min All Weather Inlet (AWI-780). The 780 L/min inlet was scaled according to its internal volume to two-thirds and one-third the original size. The smaller units were highly sensitive to wind speed.

Motivation and Objectives

In bioaerosol sampling, there is generally need for a concentrator to increase the concentration of particulate matter that is delivered to the detector or identifier. The replacement of concentration devices such as cyclones with virtual impactors has the potential to considerably reduce the overall power consumption of a biological detection system (Isaguirre, 2005). The deployment of such a system in the field that utilizes a concentration device based on virtual impaction such as a Circumferential Slot Virtual Impactor, CSVI (Haglund, 2003) would deem favorable from a power consumption standpoint.

To allow particles up to a certain size to enter the CSVI unit, an effective sampling device is necessary, which will not cause an underestimation of the concentration of particles in the size range of interest (e.g. 1 - 10 μm AD). The principal focus of this experimental study is to design, fabricate, and test an ambient sampling inlet

to be used conjointly with the CSVI unit that operates at a nominal volumetric flow rate of 100 L/min. The combined unit will allow particles to be sampled through the inlet, enter a fractionating plenum, and permit particles in a certain range of interest to gain entry to the CSVI. The sampling inlet considered herein is devoid of an internal fractionator, however, a field-worthy unit will need an internal fractionator to prevent large particles (e.g. those with sizes > 15 µm AD from entering the CSVI and potentially fouling its internal surfaces). This overall approach should provide reliable sampling to the detector or identifier that comprises particles in the range of < 15 µm AD.

In addition to the development of a 100 L/min sampler, two larger inlets, which were designed by Stokes scaling for operation at roughly 400 L/min and 800 L/min, were tested to determine their performance characteristics. The goal of this effort is to test the validity of using this approach to Stokes scaling as a concept for assisting in the design of future inlets.

The specific objectives of this study are:

- Design and fabricate an inlet capable of handling a volumetric flow rate of 100 L/min (0.00167 m^3/s), and two additional Stokes scaled versions designed to operate at 400 and 800 L/min (0.00668 and 0.01336 m^3/s). The inlets should ideally display wind independent characteristics with an overall penetration above 80% for a nominal particle size of 10 µm AD.
- Experimentally characterize the penetration of particles in the nominal size range of 5 to 20 µm AD at wind speeds of 2, 8, and 24 km/h (0.55, 2.22, and 6.67 m/s) for all inlets. Penetration characteristics will be obtained for at least four different

particle sizes for the 100 L/min inlet and three different particle sizes for the 400 and 800 L/min scaled inlets.

- Test the two larger inlets for operation at a flow rate of 1250 L/min, and conduct further aerosol tests with the unit deemed most desirable for use in a bioaerosol detection system currently fielded by the U.S. Military.

PROTOTYPE INLET DESIGNS

The inlets of this study, which shall be referred to as Bell Shaped Inlets (BSIs), have a design similar to the circumferential side entrance inlet that was developed by Wedding et al. (1977) and McFarland et al. (1979). In this type of inlet, aerosol enters the device through a circumferential intake and rises through a stilling chamber before making a U-turn and being discharged from the inlet through a concentric vertical outlet pipe. Figure 2 shows a schematic representation of the BSI design flow configuration and nomenclature of various parameters.

The vertical dimension at the intake is denoted as the intake or aspiration gap. The width of the annulus in the region between the inner and outer cylindrically shaped plena is denoted as the annular gap. The height available between the top of the inner plenum and the top of the outer plenum is referred to as the window height. The vertical distance extending from the lower flange of inner plenum to the top of the inner plenum is denoted as the rise.

A primary objective for this study is to develop a 100 L/min (0.00167 m^3/s) sampling inlet. A preliminary design for the inlet was determined by scaling a similar existing inlet (Haglund et al., 2005) designed to operate at 1250 L/min (0.021 m^3/s). A 0.305 m (12") outer plenum diameter and a 0.254 m (8") inner plenum diameter were scaled down to 0.123 m (5.2") and 0.086 m (3.4") respectively using the Stokes scaling analysis.

Two preliminary prototype designs were fabricated based on this approach; one with a 0.102 m (4") inner plenum diameter and the other with a 0.076 m (3") inner plenum diameter. These units are designated as BSI-100-4 and BSI-100-3 respectively

(Figures 3 and 4). Both units have a 0.127 m (5") outer plenum diameter. For the current study, insensitivity to wind speed and a high degree of particle penetration for a wide range of particles needs to be addressed, so it was necessary to adjust critical parameters such as the intake gap and the window height in order to achieve the desired objectives.

Following the fabrication and limited testing of the prototypes, an advanced prototype unit was fabricated by Spiral Fittings of South Carolina, Inc., a vendor that specializes in metal spinnings. The latter unit consists of an outer and inner plenum assembly, with a provision for windows at the top of the inner plenum to allow the air to pass from the annular gap to the exit tube. This unit closely resembles the BSI-100-4 and features outer and inner flange diameters of 0.222 m (8.75") and 0.210 m (8.25"). The smaller inner diameter prevents the entry of external precipitation such as rain droplets, snow or debris. This unit is designated as the BSI-100. Figures 5 and 6 show a schematic diagram and photographs of the advanced prototype inlet.

Two additional inlets, designed to operate at flow conditions of 400 L/min and 800 L/min were developed by subjecting the BSI-100 unit to a Stokes-scaling of selective parameters (Table 1). The parameters that were chosen were namely the intake or aspiration gap, the annular gap, the window height and the rise. Parameters such as the inner and outer plenum diameters and flange dimensions were not subjected to a Stokes-scaling for two reasons; one being the fact that these parameters were assumed to not have much of an effect on the overall performance and the other due to prohibitively large dimensions that would have resulted. Fabrication of these units was also provided by Spiral Fittings of South Carolina Inc. Figures 7 and 8 provide the schematic diagrams and photographs of the scaled units together with the BSI-100.

EXPERIMENTAL PROTOCOL

General

The experimental methodology for determining penetration characteristics of a sampling inlet by wind tunnel testing involves the generation of monodisperse aerosol particles, followed by collection and analysis of the desired sample. Liquid aerosol particles, generated with a vibrating orifice aerosol generator (VOAG, Model 3450, TSI Inc., St. Paul, MN) are for tests with particles larger than 3 µm AD. A combination of 9% oleic acid and 1% sodium fluorescein salt (v/m) is dissolved in 90% ethanol (v/v) to create a liquid particle master solution. After droplets are formed by the aerosol generator, the volatile ethanol evaporates leaving a residual non-volatile particle consisting of oleic acid and green fluorescent tracer. The residual droplet size is controlled by diluting the master solution while maintaining the operational parameters of the VOAG constant. Table 2 shows the recipe for obtaining 500 mL of solution that will produce droplets with sizes from 3 and 20 µm AD for operation through a 20 µm orifice. The nominal operating parameters of the VOAG for the above specified particle range include a liquid feed rate of 0.139 cm^3/min and a vibration frequency range of 40 to 80 kHz. The actual frequency is selected by trial and error in seeking to produce an aerosol with optimal monodispersity.

An important consideration when generating test aerosol is to ensure consistency of aerosol concentration and monodispersity. An Aerodynamic Particle Sizer (APS, Model 3321, TSI Inc., St. Paul, MN) is used to monitor the distribution of the generated aerosol, but it is used strictly as a tool for quality assurance. To determine the mean droplet size, the particles are impacted onto a glass slide coated with an oil-phobic agent

(Nyebar, Type Q, 2.0%, NYE Lubricants Inc., New Bedford, MA). The diameters of these impacted droplets are measured with an optical microscope. The actual size of the particles is calculated from the density of the oleic acid and fluorescein mixture (0.934 g/cm^3) and a predetermined flattening factor of 1.29 (Olan-Figueroa et al., 1982).

Once the desired size of the test aerosol is achieved, particles are sent through a 10 mCi Kr-85 charge neutralizer, which sits above the orifice, to neutralize charge that may be present on the droplets. The aerosol sample is subsequently drawn into a delivery conduit, which is a 0.86 m (34") wind tunnel duct section. Figures 9 and 10 show a schematic and photograph of the test setup. A blender or mixing element is positioned within the delivery conduit to ensure that a uniform concentration of the test aerosol arrives at the test section.

A fan and motor arrangement with a speed controller is used to force air through the wind tunnel. The air is recirculated, HEPA filtered and sent back to the intake of the fan. The centrifugal fan (Model No. 200 BSW CL 3 ARR 1, IAP, Inc., Phillips, WI) has a capacity of 4.72 m^3/s (10,000 ft^3/min) at 3 kPa (12 inches H_2O) static pressure. The motor is rated at 29.8 kW (40 hp) at 3600 rpm. A variable frequency drive (Model VLT 6042, Danfoss-Graham, Milwaukee, WI), which is used to control the motor, is rated at 29.8 kW (40 hp) and 460 volts. The three test wind speeds of 2, 8, and 24 km/h (0.55, 2.22, and 6.67 m/s) are obtained by varying the controller frequency. Wind speed at the test section is measured using a thermal anemometer (Model 8355, TSI Inc., Shoreview, MN).

Protocol for Inlet Testing

The inlet is set up at the test section of the wind tunnel, and is positioned so that the intake lies close to the horizontal mid-plane of the wind tunnel (Figure 11). It is ensured that sufficient space exists between the top of the inlet and the top of the wind tunnel to avoid excessive flow blockage. The inlet is flanked by two isokinetic nozzles, one on either side of the inlet. It is important to place the nozzles close to the intake of the inlet yet far enough to prevent flow disturbances due to the nozzles. As a rule of thumb the isokinetic nozzles are placed between the extents of the inlet intake diameter and the wall of the wind tunnel, and slightly upstream of the inlet.

During any given test, the inlet and the two isokinetic nozzles are run simultaneously for the same time duration. The tests are run long enough to ensure that the fluorescein collected on the samples exceeds the background level by at least one order of magnitude. Suggested test times vary for different wind speeds and particle sizes.

Reference aerosol samples are collected by isokinetic sampling, which ensures that the concentration at the entrance plane of the isokinetic nozzles matches that of the free stream (Hinds, 1999). Due to particle deposition occurring on the inside walls of the nozzles, the true reference concentration is calculated from the sum of the aerosol deposited on a filter placed at the exit plane of the nozzle and that deposited on the inside walls of the nozzle. Isokinetic operation of the nozzles is achieved by controlling the flow rate through the nozzle.

For the duration of each test, the aerosol particle number concentration is also monitored at the test section of the wind tunnel with an optical particle counter (Model

500, Climet Instruments, Redlands, CA). The optical particle counter provides a particle count per unit sampled volume for various particle size intervals between 1 and 15 μm AD. The optical counter, together with the aerodynamic particle sizer, provides verification of the constancy of aerosol concentration and the monodispersity of the aerosol particles.

The aerosol that penetrates through the inlet and through the isokinetic nozzles is collected on glass fiber sampling filters (Type A/D Glass Fiber Discs, Pall Corporation, East Hills, NY). For a volumetric sampling rate of 100 L/min (0.00167 m^3/s), 47 mm diameter filters are used. In the case of sampling at higher flow rates of 400, 800, and 1250 L/min (0.0067, 0.0133, and 0.0208 m^3/s), 8"x10" rectangular sheet filters are used. Samples from the isokinetic nozzles are collected on 47 mm filters.

After exposure to the aerosol, the filters are soaked in a solution of distilled water and isopropyl alcohol and left for at least six hours to ensure complete elution of the fluorescent tag from the filters. The ratio of distilled water to isopropyl is, by volume, either 1:1 or 1:2 (50%-50% or 66.7%-33.3%, v/v). The total solution volume typically used to soak a 47 mm filter is 40 or 60 mL (1:1 or 1:2), and that for an 8"x10" filter sheet is 300 mL (1:2). The inner walls of the isokinetic nozzles are also rinsed with the solution of distilled water and isopropyl alcohol (1:1 or 1:2, v/v). The solution proportion used to soak the filters was the same for any given set of tests.

The overall penetration of aerosol through an inlet can be determined from the relative concentrations of the fluorescent tracer that are measured with a fluorometer (Model 450, Sequoia-Turner, Mountain View, CA). The relative concentration for each sample may be obtained as

$$C = \frac{R \cdot V}{Q \cdot t} \quad [21]$$

where C is the relative concentration, R is the fluorometer reading adjusted for the background, V is the solution volume, Q is the air flow rate, and t is the elapsed time during which particle collection took place. The overall penetration of an inlet is then determined from:

$$P = \frac{C_{f,inlet}}{C_{f,iso} + C_{w,iso}} \quad [22]$$

where $C_{f,inlet}$ represents the relative concentration obtained from the filter of the test inlet, $C_{f,iso}$ represents the average relative concentration obtained from the filters of the two isokinetic nozzles, and $C_{w,iso}$ represents the average relative concentration obtained from the washes of the walls of the isokinetic nozzles.

UNCERTAINTY ANALYSIS

A degree of uncertainty is associated with experimental data. To have an idea of how accurate and representative the data is, it is imperative to identify the sources of uncertainty and attempt to quantify the degree to which the uncertainty occurs.

If we leave aside gross blunders in the experimental setup or instrumentation, uncertainty in experimental measurement can be classified into two categories; a) systematic or bias errors and b) precision or random errors. Systematic errors tend to appear repeatedly and cause roughly the same degree of error in the data readings. Precision errors, however, are errors that manifest in the experimental data due to random fluctuations in the apparatus or instrumentation.

One potential source of systematic error exists in any flow system used to monitor volumetric air flow rate. The presence of a leak could cause repeated inaccuracies, so it is vital to regularly check flow systems. Another type of systematic error could arise in the contamination of filters by residual fluorescein left in containers that are not properly washed, or by fluorescein transferred to the filters from contaminated objects such as tweezers, gloves, or bare hands. Containers must be washed vigorously and left to air dry, and filters should be handled in a clean environment. Systematic errors should be identified and minimized.

Due to their nature, precision errors can be quantified. These errors are generally associated with the precision of the instrumentation used to measure, for example, volumetric air flow rate, particle size, and relative fluorescence. These errors tend to propagate and cause a level of uncertainty in the calculated results.

A commonly used method for estimating uncertainty is that of Kline and McClintock (Holman, 2000). Two important parameters that require estimates of uncertainty are penetration and the Stokes number. The Kline and McClintock method defines the uncertainty associated with the calculation of a parameter *R* as

$$w_R = \sqrt{\sum_{i=1}^{n}\left(\frac{\partial R}{\partial x_i} w_i\right)^2} \qquad [23]$$

where

w_R = the uncertainty in the result *R*

x_i = independent variable with an associated uncertainty

w_i = the uncertainty in the variable x_i

n = number of independent variables with an associated uncertainty in the parameter *R*

The calculated parameters, penetration, and Stokes number may be expressed in terms of their fundamental measured quantities as follows:

$$P_{calculated} = \left[\frac{R_{\exp}}{R_{ref}}\right] \cdot \left[\frac{V_{\exp}}{V_{ref}}\right] \cdot \left[\frac{Q_{ref}}{Q_{\exp}}\right] \cdot \left[\frac{t_{ref}}{t_{\exp}}\right] \qquad [24]$$

$$Stk_{calculated} = \frac{\left(1 + \frac{2.34 \cdot \lambda}{d_p}\right) \cdot \rho_p \cdot {d_p}^2 \cdot U_o}{18 \cdot \mu \cdot d_c} \qquad [25]$$

where:

P = inlet penetration;

R = raw fluorometer reading in arbitrary units;

V = volume of total solvent used to soak filters;

Q = volumetric air flow rate;

t = test duration;

Stk = Stokes number;

λ = mean free path of air;

d_p = diameter of the test particle;

ρ_p = density of the test particle;

U_o = the undisturbed wind speed;

μ = viscosity of air;

d_c = characteristic dimension (half of the annular gap of the inlet)

The total uncertainty in inlet penetration can be estimated by incorporating individual uncertainties in the measurable quantities R, V, and Q, which represent the raw fluorometer readings, solvent volume used for soaking filters, and the total volumetric flow rates, respectively. Neglecting the error associated with the measured test time duration, the total uncertainty in inlet penetration is given as:

$$\frac{w_P}{P} = \sqrt{\sum \left(\frac{a_i w_{x_i}}{x_i} \right)^2} \qquad [26]$$

$$\text{or, } \frac{w_p}{P} = \sqrt{\left(\frac{w_{R_{\exp}}}{R_{\exp}} \right)^2 + \left(\frac{-w_{R_{ref}}}{R_{ref}} \right)^2 + \left(\frac{w_{V_{\exp}}}{V_{\exp}} \right)^2 + \left(\frac{-w_{V_{ref}}}{V_{ref}} \right)^2 + \left(\frac{-w_{Q_{\exp}}}{Q_{\exp}} \right)^2 + \left(\frac{w_{Q_{ref}}}{Q_{ref}} \right)^2} \qquad [27]$$

Here a_i is the exponent of each variable x_i. If the uncertainties associated with R, V, and Q are assumed to be 5%, 1.25%, and 5%, respectively, the total uncertainty in the calculated value of inlet penetration is estimated to be 10.2%.

The uncertainty in the Stokes number is given in general form by

$$w_{Stk} = \sqrt{\sum \left(\frac{\partial Stk}{\partial x_i} w_{x_i} \right)^2} \qquad [28]$$

The measured variables which contribute to the total uncertainty are the particle diameter d_p, wind speed U_o, and the characteristic dimension d_c. All other parameters are such as the mean free path of air λ, viscosity of air μ take values that are present in existing text and the errors associated with these values are assumed to be negligible.

If we rewrite the Stokes number as,

$$Stk = \frac{(d_p{}^2 + 2.34 \cdot \lambda \cdot d_p) \cdot \rho_p \cdot U_o}{18 \cdot \mu \cdot d_c} \qquad [29]$$

and partially differentiate with respect to the concerned variables, we arrive at the following results:

$$\frac{\partial Stk}{\partial d_p} = \left(\frac{2 \cdot d_p + 2.34 \cdot \lambda}{d_p + 2.34 \cdot \lambda} \right) \cdot \frac{Stk}{d_p} \qquad [30]$$

$$\frac{\partial Stk}{\partial U_o} = \frac{Stk}{U_o} \qquad [31]$$

$$\frac{\partial Stk}{\partial d_c} = -\frac{Stk}{d_c} \qquad [32]$$

The uncertainty in calculating the Stokes number for a given particle size can then be expressed as

$$\frac{w_{Stk}}{Stk} = \sqrt{\left[\left(\frac{2 \cdot d_p + 2.34 \cdot \lambda}{d_p + 2.34 \cdot \lambda} \right) \cdot \left(\frac{w_{d_p}}{d_p} \right) \right]^2 + \left(\frac{w_U}{U_o} \right)^2 + \left(\frac{w_{d_c}}{d_c} \right)^2} \qquad [33]$$

The uncertainty in measuring the particle size d_p is estimated to be 4%, 2%, 1%, and 1% for nominal particle sizes of 5, 10, 15, and 20 μm AD, respectively, while the errors associated in measuring the velocity U_o, and the characteristic dimension (inlet annular gap) d_c are 3% and 0.2%. The total predicted uncertainty in the calculated value of the

Stokes number is 8.4%, 5%, 4% and 3.6% for the nominal particle sizes mentioned above.

QUALITY ASSURANCE

Quality of Test Aerosol

The quality of the test particles is given suitable consideration in terms of its sizing, monodispersity, and uniformity of concentration at the test section. Particle sizing is carried out by impacting the test particles onto microscopic slides coated with an oil-phobic fluorocarbon surfactant (Nyebar, Type Q, 2.0%, NYE Lubricants Inc., New Bedford, MA). The particles are observed with the aid of an optical microscope that is calibrated by a stage micrometer. It is ensured that particles chosen for measurement lie on the periphery of the impacted sample to avoid measurement of doublets. Several particles are measured before taking an average size reading.

The aerodynamic particle sizer and optical particle counter assure that the test aerosol being released from the aerosol generator and arriving at the test section is monodisperse. These instruments monitor the aerosol throughout the duration of each test. A test is rejected if during the test, there appear an inordinate fraction of satellite particles (greater than 10% multiplets), and the VOAG may need adjustment before continuing.

A uniform concentration of aerosol in the wind tunnel near the test section is critical for acquiring accurate performance data. Two isokinetic nozzles are run as references simultaneously with the sampling inlet. An average reading from the two nozzles is used as the reference reading in order to eliminate any variation in particle concentration across the test plane. Test durations are long enough to ensure that the fluorescein collected on the filters is at least one order of magnitude greater than the

background fluorescein level. All data points presented in this study are represented as the average of at least three test runs for a given operating condition.

Flow and Velocity Measurement

All rotameters and flow measuring equipment are calibrated and checked for leaks prior to testing. A thermal anemometer (VelociCalc, Model No. 8355, TSI Inc., Shoreview, MN) is used for measuring velocity in the wind tunnel. Rotameters (Dwyer Instruments, Michigan City, IN) are used for monitoring flow rates and are calibrated with a Roots Meter (Model 5M 125 TC, Dresser Measurement, Houston, TX) for assurance of accuracy. The reading obtained from the rotameters is corrected for the pressure drop through the system, as follows.

$$Q_{actual} = Q_{read} \times \sqrt{\frac{p_a - \Delta p}{p_a}} \qquad [34]$$

Where Q_{actual} is the actual volumetric flow rate; Q_{read} is the observed volumetric flow rate; p_a is the atmospheric barometric pressure; and Δp is the pressure drop in the system. While testing inlets, the filter media causes a significant pressure drop to occur in the system. To overcome the pressure drop, compensation must be made to ensure that the flow rate upstream of the filter being pulled through the inlet is the true flow. The system pressure drop is measured using Magnehelic differential pressure gauges (Dwyer Instruments, Michigan City, IN).

Fluorometric Analysis

The fluorescein concentrations from the collected inlet and reference samples are quantified using a fluorometer (Model 450, Turner-Sequoia, Mountain View, CA). Many

factors influence the fluorometric analysis including wavelength and intensity of primary light, and the transmission characteristic of the excitation and emission filters that are used in the instrument. Kesavan et al. (2001) observed that the stability of the fluorescent material can be disturbed by small changes in physical and chemical parameters, such as the pH, ionic state of the molecule, nature of the solvent, viscosity, temperature, etc. The optimum excitation and emission wavelengths are found to be 492 nm and 516 nm. The fluorescent solution is also strongly pH dependent, but for values above 9, the intensity is both maximized and constant. Use of the NB490 and SC515 filters and adding one drop of 1N NaOH for every 5 mL of liquid sample satisfies the quality issues for the fluorometric analysis.

RESULTS AND DISCUSSION

Wind tunnel tests with liquid particles serving as the test aerosol were conducted on the inlets described. Tests were conducted with a focus on determining inlet aerosol penetration as a function of particle size for wind speeds of 2, 8, and 24 km/h.

BSI-100-4 and BSI-100-3 Prototype Units

Tests were conducted with the BSI-100-4 and BSI-100-3 prototype units to provide a basis for speculating on the feasibility of meeting the essential inlet design objectives. These inlets were tested without either a bug screen or an internal fractionator. The performance of each of these units is plotted as a function of wind speed for a particle size of 10.6 µm AD in Figure 12. The performance characteristics were then obtained for a range of intakes or aspiration gaps and the window height. The variation of these parameters is found to influence inlet performance at 24 km/h. Figures 13 and 14 show the effect of different intake gaps on the performance of both inlets. Penetration improves (increases) as the intake gap is increased, probably as a result of reduced aerosol particle impaction on the inlet walls in the gap region. The BSI-100-4 and BSI-100-3 units with intake gaps of 0.023 m (0.9") and 0.036 m (1.4"), respectively indicate acceptable performance levels in terms of insensitivity to wind speed for a particle size of 10.6 µm AD.

Once the geometries were fixed, each prototype was run for four different particle sizes ranging from 5 to 18 µm AD. Penetration as a function of particle size for all three wind speeds is shown for the BSI-100-4 and BSI-100-3 in Figures 15 and 16. Both units display particle penetration above 80% at all three wind speeds for a particle size of 11.2

µm AD. Penetration decreases, particularly at a wind speed of 24 km/h, for particle sizes larger than 11.2 µm AD.

BSI-100 Advanced Prototype Unit

Aerosol testing was carried out on an advanced prototype BSI-100 unit fabricated by Spiral Fittings Inc. of South Carolina. This inlet closely resembles the BSI-100-4 unit and was extensively characterized for different wind speeds and particle sizes. Figure 17 shows penetration as a function of wind speed for a particle size of 10.1 µm AD. As anticipated, results are similar to those presented in Figure 12 for the BSI-100-4 prototype unit.

Initial testing on the BSI-100 unit was carried out without a bug screen. Screens are critical components that need to be incorporated into an inlet to preclude the entry of insects, lint, and large debris into the aerosol sampling system. Tests on the BSI-100 were conducted with various screens placed horizontally at a location just below the windows of the inner plenum. The two screens were tested, namely a coarse 8-mesh, 0.432 mm (0.017") wire diameter screen and a finer 16-mesh, 0.229 mm (0.009") wire diameter screen. Figure 18 shows the effect of different screens on the performance of the inlet over three wind speeds and for a particle size of 10.5 µm AD. It is observed that the curves are parallel indicating that the screen losses are not greatly affected by changes in wind speed.

Penetration results were obtained for five different particle sizes between 5 and 16 µm AD and plotted for three wind speeds (Figure 19). The penetration curves for all three wind speeds are similar to the results obtained for the BSI-100-4 unit. A particle

size of 6 µm AD displays 100% penetration for all wind speeds, whereas for the largest test particle of 15.5 µm AD, penetration is between 75% and 80% for 2 and 8 km/h, and 25% for 24 km/h. It is evident from these data that particle deposition via impaction onto the internal surfaces of the inlet is more prominent for particles with higher inertia.

Another performance metric that has been examined in this study is inlet penetration as a function of the operating flow rate. This provides an insight into the range of application of the inlet or its performance at off-design conditions. Figure 20 shows inlet penetration varying with the operating flow rate for a wind speed of 8 km/h and a particle size of 10.4 to 10.7 µm AD. Tests were conducted for five different flow rates between the design flow condition of 100 L/min and up to a maximum of 1250 L/min. Performance is stable and constant up to 800 L/min, but a reduction in penetration is observed for the flow rate of 1250 L/min.

Stokes-Scaled Units

Tests were conducted to explore the validity of the Stokes-scaling approach in the design of inlets. Two scaled units were fabricated to accommodate design flow rates of 400 and 800 L/min. These units are designated as BSI-400 and BSI-800, respectively.

Tests were run devoid of a screen and fractionator for the BSI-400 and BSI-800. Figures 21 and 22 show penetration plotted as a function of wind speed for the two scaled units operating at their design flow rates for a particle size of 10.5 µm AD. Performance data is plotted at design conditions for the two scaled units along with the BSI-100 for comparison in Figure 23. It is observed that the selected method of Stokes scaling collapses the data within a 90% to 100% penetration band for all three units.

Penetration characteristics of the BSI-400 and BSI-800 were determined for five different particle sizes ranging from 5 to 22 µm AD and three wind speeds of 2, 8, and 24 km/h (Figures 24 and 25). Each unit was operated at its design flow rate. Results indicate performance of the BSI-400 and BSI-800 similar to that of the BSI-100. Penetration for both scaled units exceeds 80% at all three wind speeds for a particle size of about 13 µm AD, compared to 11.5 µm AD for the BSI-100.

The effect of varying the flow rate was observed for the BSI-400 and BSI-800 units. Figures 26 and 27 show the effect of flow rate on the penetration of the BSI-400 and BSI-800, respectively, at a wind speed of 8 km/h. Flow rates were varied from a minimum flow of 50% of the design flow rate and up to a maximum of 1250 L/min. It can be seen that maximum penetration tends to occur at the design flow rate. Penetration is observed to decline above and below the design point.

For a comparison of the BSI series inlets, their performances are plotted as a function of the Stokes number, which is based on the free stream velocity and the characteristic dimension, d_c of half of the annular gap for each inlet. The undisturbed velocity, U_o, is taken to be the ambient wind speed of 2, 8, or 24 km/h, which has an effect on inlet performance. Penetration as a function of Stokes number for all three inlets is plotted separately at 2, 8, and 24 km/h wind speeds (Figures 28 to 30). It is observed that although the performances for all three inlets follow a similar trend, wind speed has an effect on the Stokes number at which the curves break downwards, which raises a question on the utility of solely relying on Stokes-scaling to improve the inlet design process.

Application of the Modified Velocity Ratio

A modified velocity ratio has been suggested for omnidirectional inlets. The non-dimensional velocity ratio U^*/U_o is plotted as a function of wind speed for various inlets in Figure 31. The inlets included in the plot are the BSI inlets, a currently field-deployed inlet that operates at 780 L/min, and the UCI-1250 which is essentially the BSI-400 unit operating at upgraded flow rate of 1250 L/min.

The analysis presented above showed that simple Stokes-scaling fails to sufficiently capture the complexity of inlet performance. This is likely because it misses the interaction of two independent flow fields (sampling flow and ambient wind speed). The use of a modified Stokes number for inlets – one based on the free stream – attempts to provide an alternative model, by drawing a relation between particle behavior and ambient wind speed. Another equally vital aspect of this model is the interaction of the free stream with the internal inlet flow (an attribute of the sampling flow rate), which is accounted for by including the modified velocity ratio in the model. Using the Stokes number based on the free stream, denoted as Stk_{FS}, and the modified velocity ratio, U^*/U_o, we can present the performance data for all three BSI units for all three wind speeds on a single graph.

Figure 32 shows a scatter of experimental values of penetration plotted as a function of Stk_{FS} using a grouping scheme that organizes inlets by series and wind speed where each group has a unique color and symbol. Each BSI unit at a given wind speed, can be associated with a modified velocity ratio value, which has been incorporated into a correlation equation describing the functional relationship between penetration, the Stokes number based on the free stream, and the modified velocity ratio. The correlation

equation representing the BSI series is presented below and plotted together with the experimental data scatter.

$$P = 100 + \left(\frac{U^*}{U_o} - 1\right) \cdot \left[31 + 2085 \cdot \left(\frac{U^*}{U_o}\right)\right] \cdot Stk_{FS} \qquad [35]$$

It is observed that the results indicate a progressive trend in reduction of inlet penetration with increasing Stokes number and velocity ratio. For a given value of Stokes number, inlet penetration increases for a decrease in the velocity ratio. Also, for small values of Stokes number, the penetration curves approach unity independent of velocity ratio.

The observations described above offer the possibility for prediction of inlet performance and an improved design procedure. To elucidate on the usefulness of the result, let us assume a hypothetical BSI inlet for design to operate at say, 600 L/min. The basic design approach and procedure to predict performance is outlined as follows. The BSI-600 geometry can be obtained from the Stokes scaling factor, and modified velocity ratios for three wind speeds determined based on the geometry. The inlet's performance can finally be predicted by using each velocity ratio and plotting penetration over a Stokes number range according to Equation 35.

Upgrade Effort

In its present configuration, the field sampling system deployed by the U.S. military operates at 780 L/min, but efforts are being devoted to increasing the flow rate to 1250 L/min.

The BSI series of inlets were speculated as candidates for an inlet worthy of acceptable performance at 1250 L/min. This would entail a high degree of aerosol

penetration and insensitivity to wind speed for a nominal particle size of 10 µm AD. Figure 33 shows how each of the BSI units perform at a flow rate of 1250 L/min, and how they compare to the presently deployed system inlet operating at 780 L/min. Results are plotted for penetration as a function of wind speed for a particle size of 10.6 µm AD. It should also be noted that tests on the BSI units were conducted without any screens, whereas the data for the JBPDS inlet indicates the presence of a screen.

Results indicate that performance of the BSI-400 and BSI-800 has high penetration and wind-independent characteristics. The BSI-400 has been selected over the BSI-800 as a candidate due to its considerably smaller size, and the BSI-400 operating at 1250 L/min is denoted as the UCI-1250.

Flow Visualization

A flow visualization study was conducted using smoke to gain qualitative insight into the flow fields within the BSI inlet. A BSI-400 unit was modified using a clear outer plenum cover and a means to allow light to enter the inner plenum to enhance visibility. The BSI-400 unit was run for flow rates of 200, 400, 800, and 1250 L/min, while smoke was allowed to enter at a single circumferential location. The visualization was conducted with smoke entering the inlet in a static condition, with no ambient wind speed.

Figures 34 to 37 depict flow patterns within the BSI-400 unit for flow rates of 200 to 1250 L/min. The region under observation is the space at the top of the inlet between the outer and inner plenum where the flow makes an 180^{o}-turn through the windows. It is seen that as the flow rate increases, the turn radius increases and the turbulence

becomes more intense. At flow rates of 200 and 400 L/min, the smoke is seen to make a well-defined, sharp turn. At higher flows of 800 and 1250 L/min, the turn radius is larger and the smoke is seen to be more dispersed effecting possible particle loss on surfaces of the inner plenum.

Interfacing with a CSVI

The primary effort of the current study is to be able to develop an inlet that collects a sample to be presented to a Circumferential Slot Virtual Impactor (CSVI). A CSVI plenum with a particle cup impactor, to separate the coarse particles from the fine, would be placed downstream of the inlet.

A compact design for the plenum was considered, which has a basic shell body dimension of 0.152 m (6") (Figure 38). This assembly also includes an annular piece that rests just below the receiver of the CSVI unit and smoothly guides the aerosol to the circumferential entry. This design uses a bolt pattern on the CSVI base for external attachment.

Aerosol tests were conducted on the plenum assembly on a setup that consisted of a mixing plenum that simultaneously delivers aerosol to a sample tube and a reference tube. A CSVI devoid of the receiver blades had spacers placed to represent the true CSVI entrance gap. 100 L/min was pulled through the minor flow tube while the major flow ports were blocked.

The plenum was tested with three impaction jet nozzle diameters of 0.025 m (1"), 0.032 m (1.25"), and 0.037 m (1.45") over a particle size range of 7 to 18 μm AD. The results depicted in Figure 39 suggest satisfactory penetration characteristics with no

significant loss of particles. Test results for the plenum show the cutpoints of the jets to be 11.1, 13.6, and 16.3 μm for the 0.025, 0.032, and 0.037 m jets, respectively.

SUMMARY AND CONCLUSIONS

The current study is aimed at designing, fabricating, and testing an inlet suitable for operation at a volumetric flow rate of 100 L/min to be used in conjunction with a CSVI bioaerosol concentrator. This task was motivated by the fact that the CSVI could considerably reduce overall power consumption and make it worthy for field deployment in a battery-operated mode.

The BSI-100 inlet was the inlet of choice for development as it displayed wind independent penetration characteristics close to 90% at all three wind speeds 2, 8, and 24 km/h for a nominal particle size of 10 µm AD. The BSI-100 inlet is also capable of displaying penetration characteristics above 80% at all three wind speeds for aerosol particles up to 11.5 µm AD. The ability to sample a high degree of particles up to that size range is favorable considering that the CSVI would be compatible with an inlet having a cutpoint close to 11 µm AD. The BSI-100 is therefore observed to be an efficient sampler that improves the overall reliability of the sampling system by minimizing particle loss and sensitivity to external factors like wind velocity.

The BSI-100 inlet is also seen to have a wide range of application in terms of its variation with the volumetric sampling rate. The inlet was able to handle penetration above 90% at 8 km/h for flow rates up to 800 L/min. This presents scope for the BSI-100 to suit alternate system requirements while maintaining a high degree of penetration.

A rigorous analytical design approach fails to exist which is the reason why inlet design has been a topic of uncertainty. An attempt was made to implement and validate the use of Stokes-scaling to assist in the future design of inlets. Two additional inlets, the BSI-400 and the BSI-800 operating at 400 and 800 L/min, respectively, were developed

and scaled from the BSI-100 configuration. Results indicate that at the design flow rates, all three units performed similarly. When penetration was plotted as a function of wind speed for a nominal particle size of 10 µm AD, the BSI inlets all performed within a 90% to 100% band. Particle size characteristics were also similar in terms of the selection curves for three wind speeds. The BSI-400 and BSI-800 units have the ability to sample with a penetration above 80% at all three wind speeds up to a particle size of 13 µm AD, compared to 11.5 µm AD for the BSI-100.

It is observed from the study that the results obtained from the plots of penetration versus Stokes number for all BSI units suggests that we cannot solely rely on using only Stokes-scaling for designing inlets. A likely reason is that it fails to capture the complexity of the dynamic model associated with inlets, which involves the interaction of two independent velocity fields. The use of a modified Stokes number based on the free stream wind speed is only partly representative of the dynamics associated with inlets. It is imperative to introduce a parameter that represents the interaction of the external flow field with the internal inlet flow, described by the modified velocity ratio. When the results were summarized for all inlets at all wind speeds, a noticeable trend emerged with respect to the velocity ratio. A model to predict inlet performance was developed, using a correlation equation to describe the BSI family of curves. This provides promise for improving the overall design process not only for inlets of the BSI design style, but possibly for the design of other omnidirectional inlets.

Although the designed operating points of the BSI inlets were fixed, it was profitable to determine their performance at a higher flow rate of 1250 L/min to suit the upgrade requirements of the point detection system specifications. The BSI-400 and

BSI-800 clearly met the expected requirements and it was the smaller BSI-400 unit that was chosen for further development. When operated at 1250 L/min, the BSI-400 showed wind independent penetration of close to 90% at three wind speeds of 2, 8, and 24 km/h and for a nominal particle size of 10 µm AD.

REFERENCES

Agarwal, J.K. (1972). The Sampling of Aerosol. Report # 208, Particle Technology Laboratory, University of Minnesota, Minneapolis, MN.

Davies, C.N. (1968). Entry of Aerosols into Sampling Tubes and Heads, *British Journal of Applied Physics.* 1:921-932.

Haglund, J.S., Ortiz, C.A., Hu, S., Seo, Y., Thien, B.F., McFarland, A.R. (2005). JBPDS Sampling System Upgrade Project: Feasibility of Improving Performance. July Report, Aerosol Technology Laboratory, Texas Engineering Experiment Station, Texas A&M University, College Station, TX.

Haglund, J.S. (2003). *Two Linear Slot Virtual Impactors for Concentration of Bioaerosols*, Ph.D. Dissertation, Department of Mechanical Engineering, Texas A&M University, College Station, TX.

Hinds, W.C. (1999). *Aerosol Technology,* John Wiley and Sons, Inc., New York.

Holman, J.P. (2000). *Experimental Methods for Engineers,* McGraw-Hill Mechanical Engineering, New York.

Isaguirre, R.R. (2004). *A 100 L/min Circumferential Slot Virtual Impactor for Bioaerosol Concentration,* M.S. Thesis, Department of Mechanical Engineering, Texas A&M University, College Station, TX.

Kesavan, J., Doherty, R.W., Wise, D.G., and McFarland, A.R. (2001). Factors that Affect Fluorescein Analysis. Final Report ECBC-TR-208, Edgewood Chemical Biological Center, U.S. Army Soldier and Biological Chemical Command, Edgewood, MD.

Liu, B.Y.H. and Pui, D.Y.H. (1981). Aerosol Sampling Inlets and Inhalable Particles. *Atmospheric Environment.* 15:589-600.

McFarland, A.R., Ortiz, C.A., and Ripps, G.J. (1978). Sampling Characteristics of the Beckman Dichotomous Sampler. Report # 3580/07/01/ARM, Air Quality Laboratory, Texas A&M University, College Station, TX.

McFarland, A.R., Ortiz, C.A., and Rodes, C.E. (1979). Characteristics of Aerosol Samplers Used in Ambient Air Monitoring. Paper presented at the 86th National Meeting of the American Institute of Chemical Engineers, April 1-5, 1979, Houston, TX.

McFarland, A.R. and Ortiz, C.A. (1982). Characterization of Sierra-Andersen PM-10 Inlet Model 246B. Report # 16/02/02/84/ARM, Texas A&M University, College Station, TX.

Olan-Figueroa, E., McFarland, A.R., and Ortiz, C.A. (1982). Flattening coefficients for DOP and oleic acid droplets deposited on treated glass slides. *American Industrial Hygiene Association Journal.* 43:395-399.

Seo, Y. (2004). *Degree of Mixing Downstream of Rectangular Bends and Design of Inlets for Ambient Bio-Aerosol Sampling.* M.S. Thesis, Department of Mechanical Engineering, Texas A&M University, College Station, TX.

Stevens, R.K., Dzubay, T.G., Russworm, G., and Rickel, D. (1977). Sampling and Analysis of Atmospheric Sulfates and Related Species. *Atmospheric Environment.* 12:55-68.

Tolocka, M.P., Peters, T.M., Vanderpool, R.W., Chen, F., and Wiener, R.W. (2001). On the Modification of the Low Flow-Rate PM_{10} Dichotomous Sampler Inlet. *Aerosol Science and Technology.* 34:407-415

Wedding, J.B., McFarland, A.R., and Cermak, J.E. (1977). Large Particle Collection Characteristics of Ambient Aerosol Samplers. *Environmental Science and Technology*. 11:387-390.

Wedding, J.B. (1982). Ambient Aerosol Sampling. History, Present Thinking, and a Proposed Inlet for Inhalable Particulate Matter. *Environmental Science and Technology*. 16:154-161

Wolf, W.P. and Hohe, D.R. (2000). JBPDS Block I EMD Program Overview and Summary, *Proceedings of the 1st Joint Conference on Point Detection for Chemical and Biological Defense,* Williamsburg, VA.

Other Sources Consulted

Fatah, A.A., Barrett, J.A., Arcilesi Jr., R.D., Ewing, K.J., Lattin, C.H., and Moshier, T.F. (2001). An Introduction to Biological Agent Detection Equipment for Emergency First Responders. National Institute of Justice Guide 101-00. Retrieved from http://www.ncjrs.org/pdffiles1/nij/190747.pdf.

Knobler, S.L., Mahmoud A.A.F., and Pray, L.A. (2002). *Biological Threats and Terrorism, Assessing the Science and Response Capabilities: Workshop Summary.* National Academy Press, Washington, DC.

Rosen, P. and Committee Members (1999). *Chemical and Biological Terrorism, Research and Development to Improve Civilian Medical Response.* National Academy Press, Washington, DC.

APPENDIX A

TABLES

Table 1: Summary of characteristic dimensions for each Stokes-scaled inlet corresponding to selective critical BSI-100 parameters.

	100 L/min	400 L/min	800 L/min
Parameter	**BSI-100 Characteristic Dimension (m)**	**Scaled characteristic dimension (m)**	**Scaled characteristic dimension (m)**
Aspiration gap	0.023	0.036	0.046
Annular Gap	0.013	0.020	0.025
Window Height	0.038	0.060	0.076
Rise	0.125	0.199	0.251

Table 2**:** Particle sizing approximation chart for VOAG solution used through a 20 µm orifice. Nominal VOAG operating parameters include a liquid feed rate of 0.139 cm^3/min and a vibration frequency range of 40 to 80 kHz.

Approximate Particle Size (µm)	Oleic Acid/Fluorescein Master (mL)	Ethanol (mL)	Total Solution Vol (mL)
3	1	499	500
4	4	496	500
5	7	493	500
6	12	488	500
7	19	481	500
8	28	472	500
9	40	460	500
10	55	445	500
11	74	426	500
12	96	404	500
13	122	378	500
14	152	348	500
15	187	313	500
16	227	273	500
17	272	228	500
18	323	177	500
19	380	120	500
20	443	57	500

APPENDIX B

FIGURES

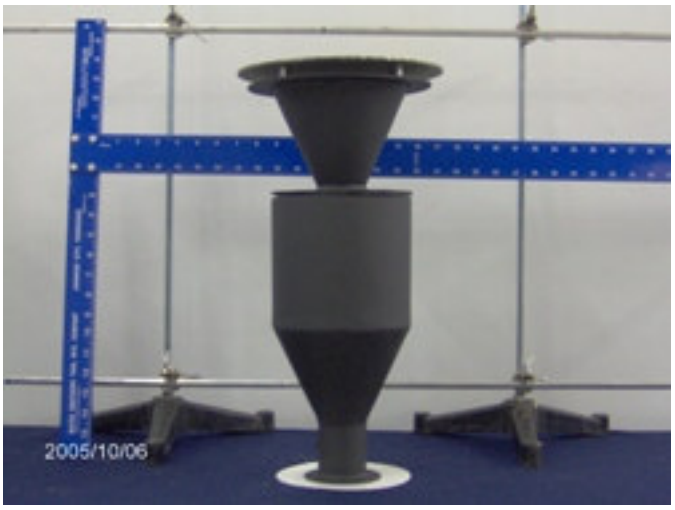

Figure 1: Example of an inlet used on a biological point detection system.

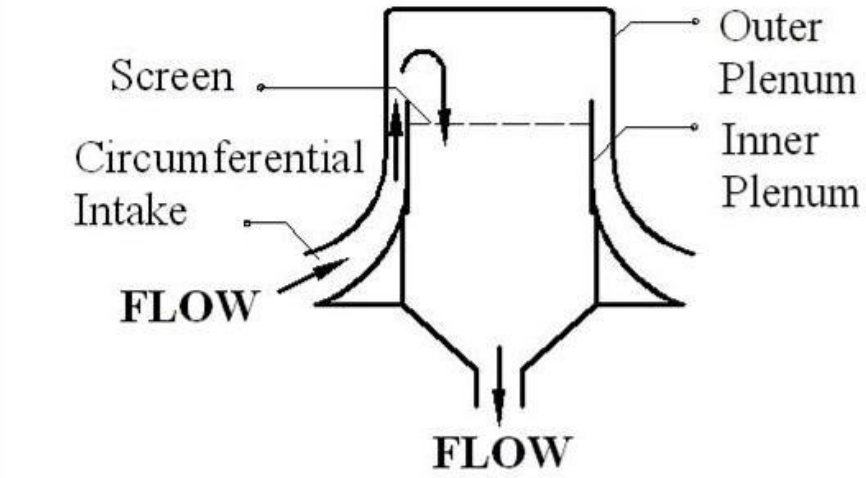

(a)

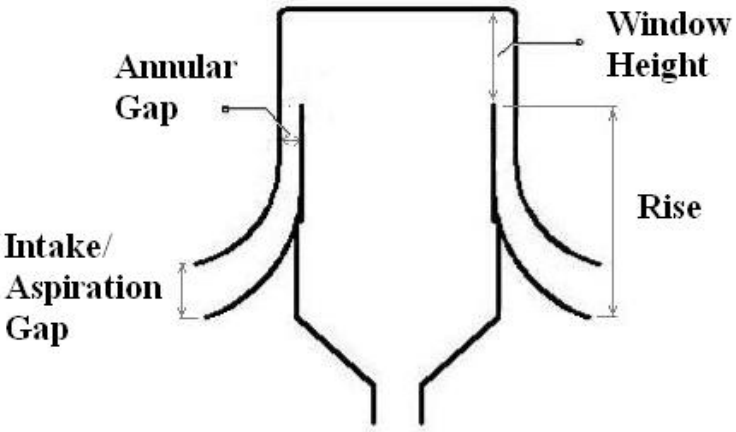

(b)

Figure 2: Schematic of the BSI design showing (a) flow configuration and (b) nomenclature of various parameters.

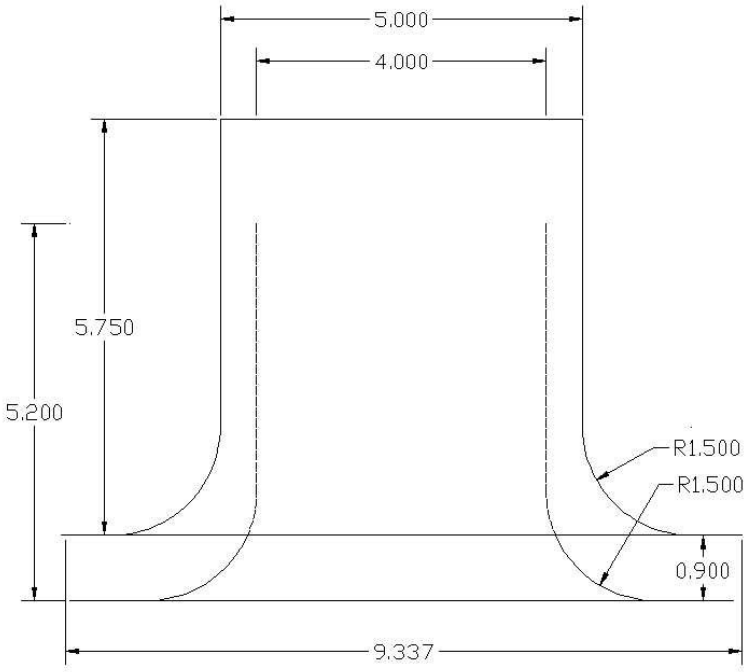

Figure 3: BSI-100-4 prototype schematic.

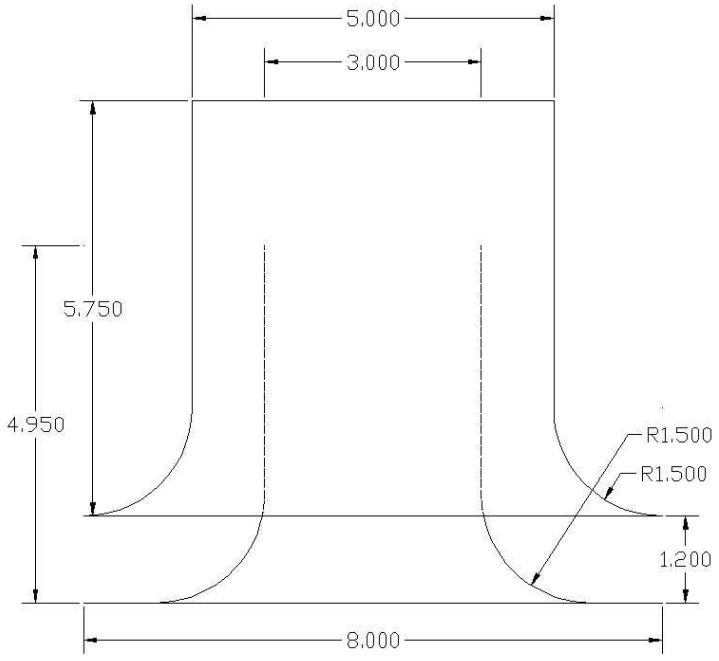

Figure 4: BSI-100-3 prototype schematic.

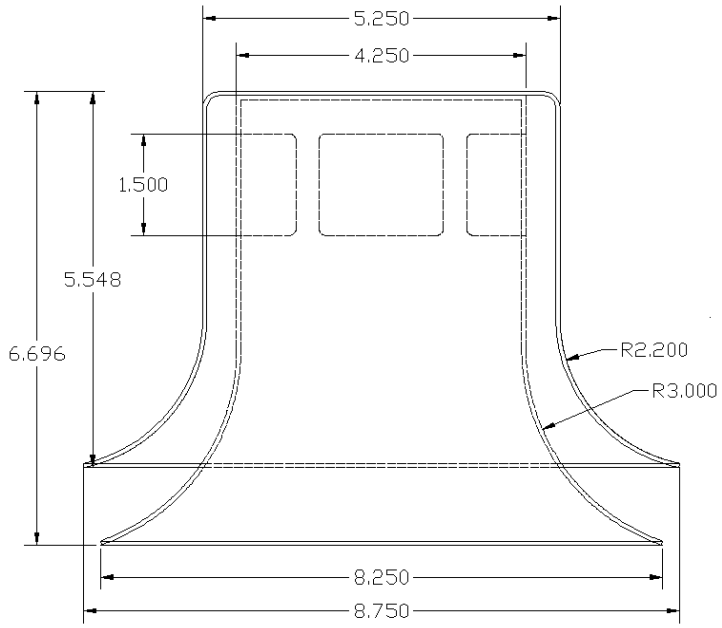

Figure 5: Schematic of the BSI-100 advanced prototype unit.

Figure 6: BSI-100 advanced prototype assembly.

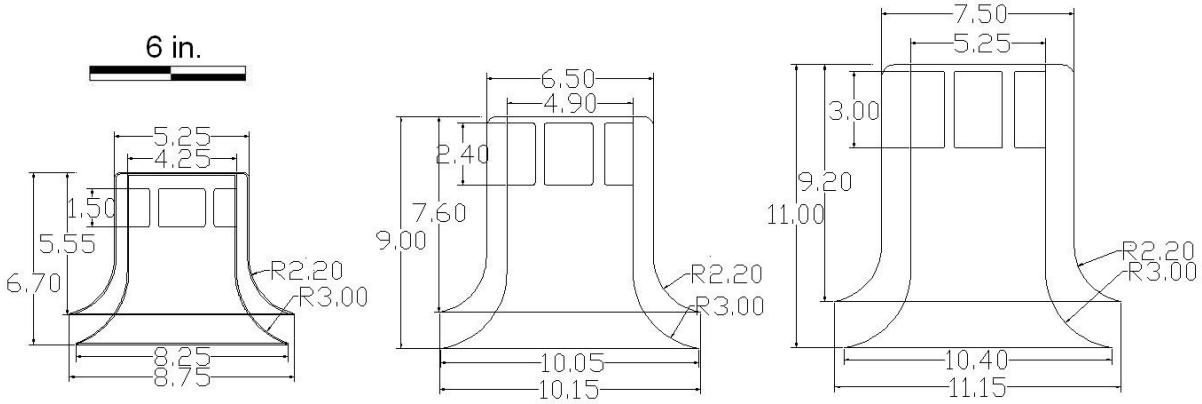

Figure 7: Schematic of the BSI-100, BSI-400, and BSI-800 units (shown to scale).

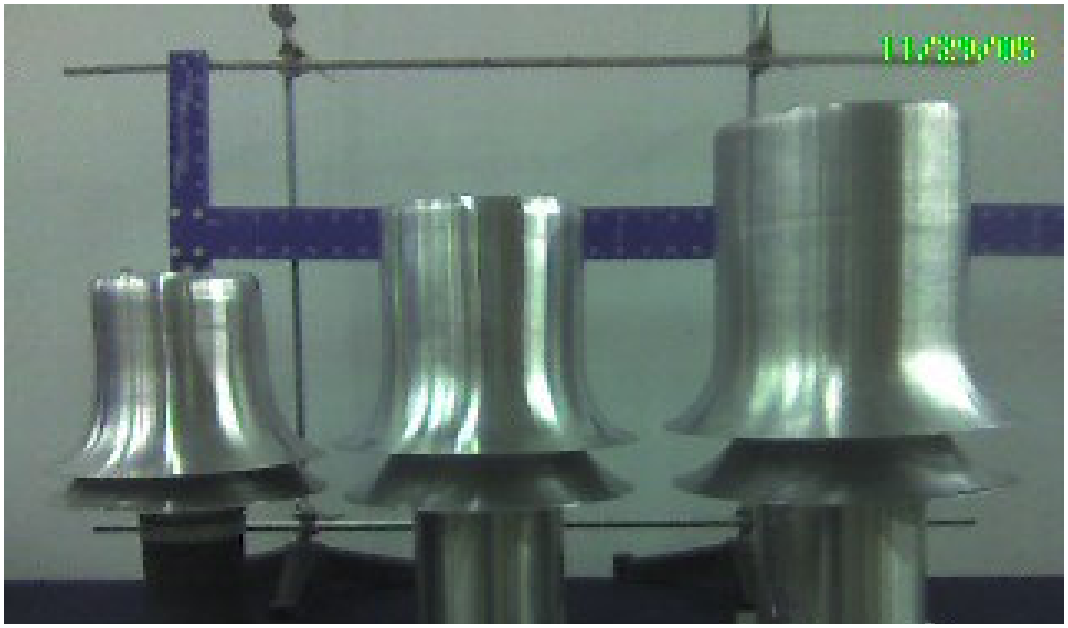

Figure 8: Photograph of the BSI-100, BSI-400, and BSI-800 units.

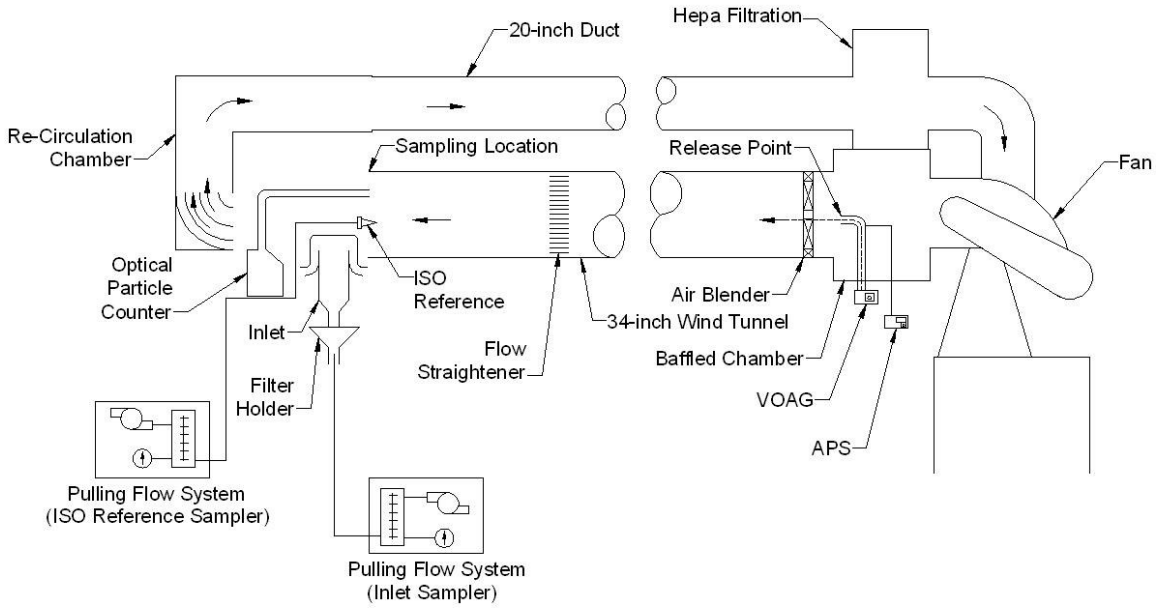

Figure 9: Schematic of the general test setup.

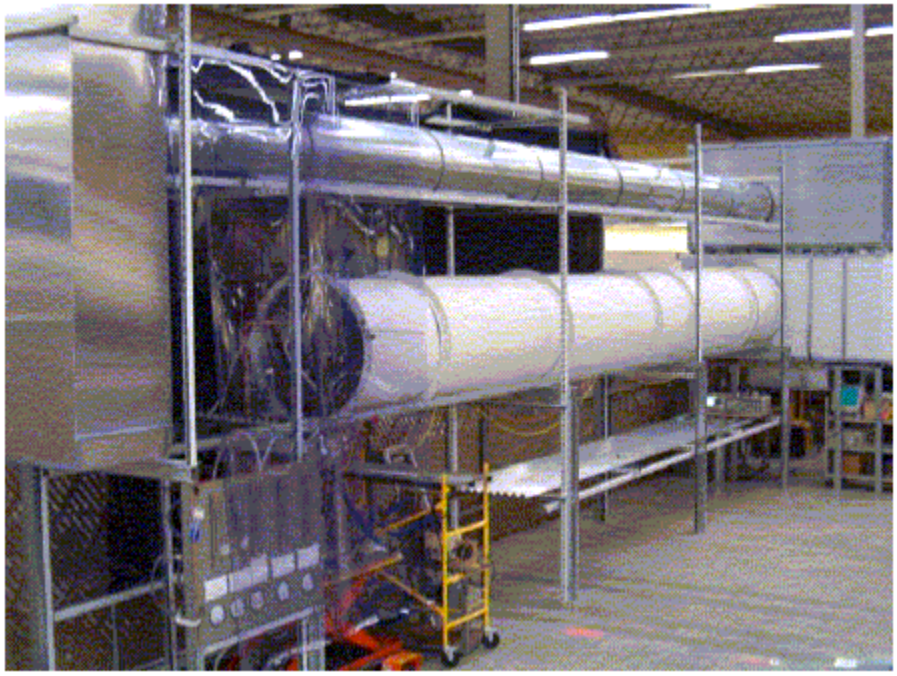

Figure 10: Photograph of the wind tunnel facility.

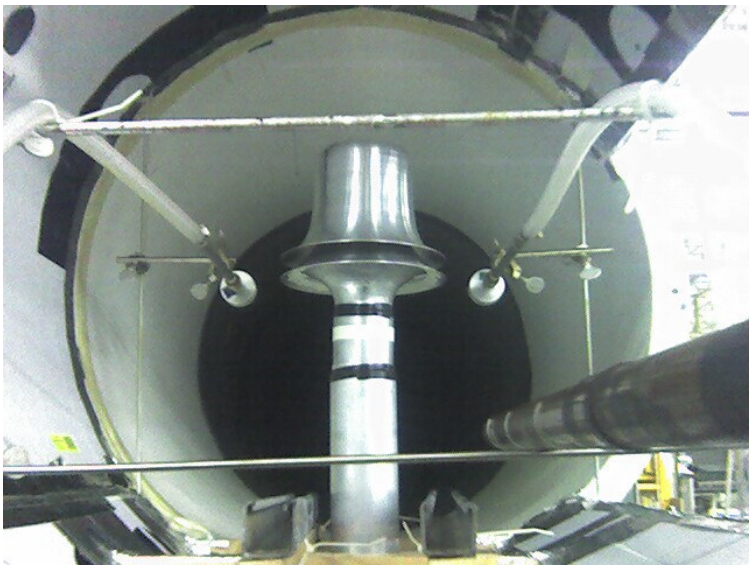

Figure 11: Photograph showing placement of inlet and reference nozzles in wind tunnel test section.

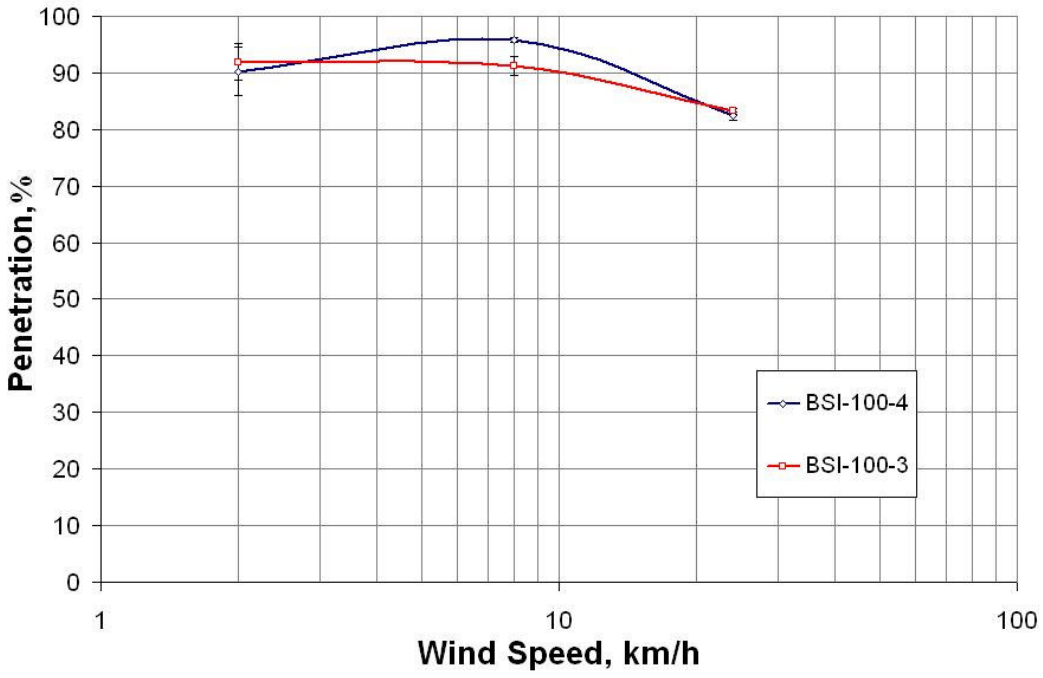

Figure 12: Penetration as a function of wind speed for the BSI-100-4 and BSI-100-3. Particle size: 10.6 µm AD.

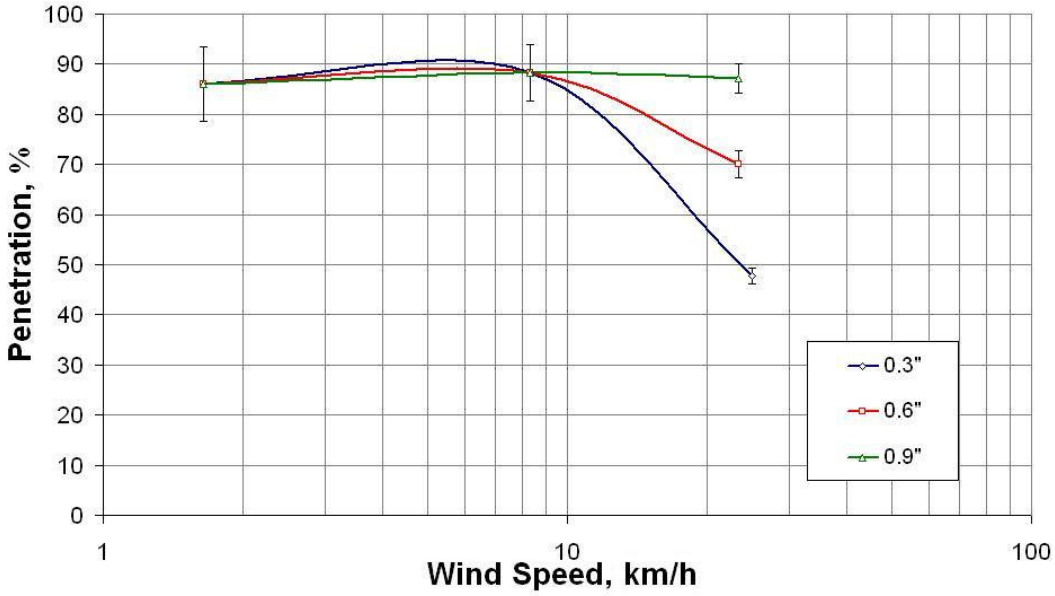

Figure 13: BSI-100-4, penetration as a function of wind speed for various intake gaps at 24 km/h. Particle size: 10.6 µm AD.

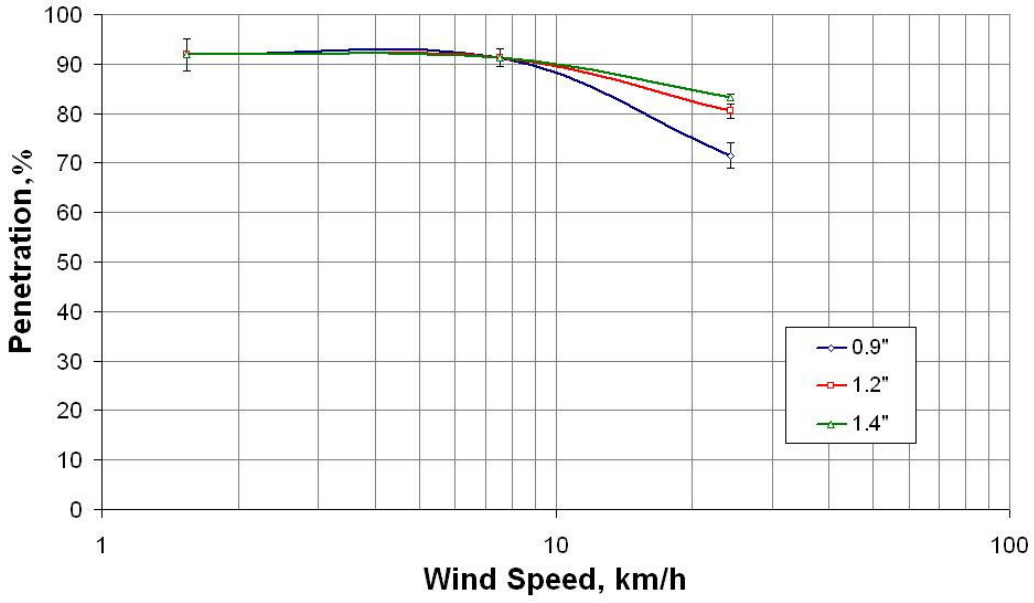

Figure 14: BSI-100-3, penetration as a function of wind speed for various intake gaps at 24 km/h. Particle size: 10.6 µm AD.

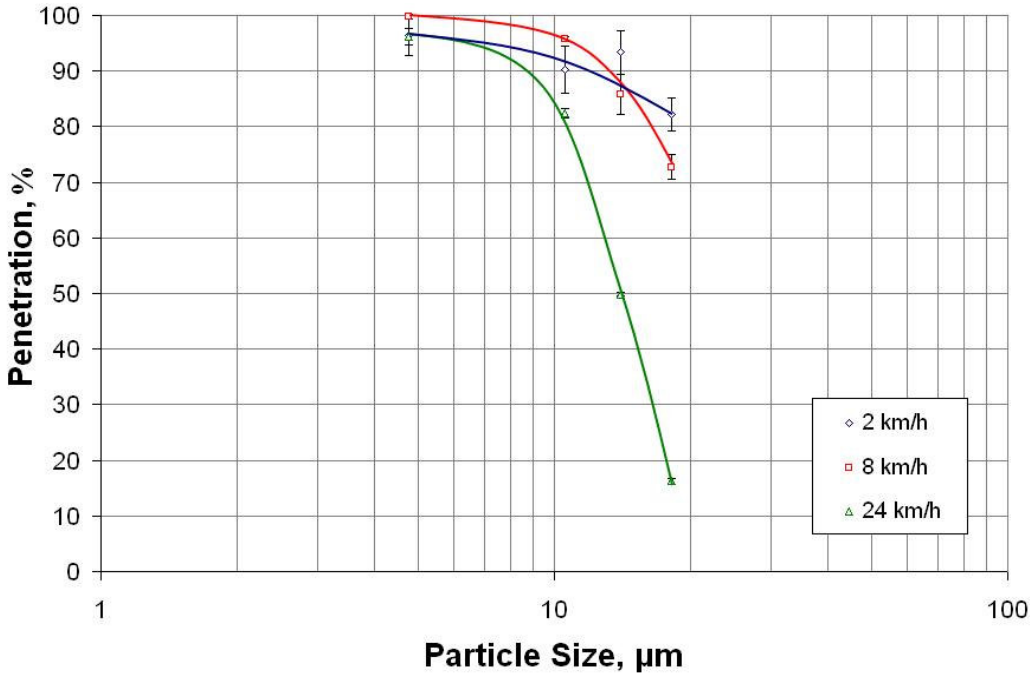

Figure 15: BSI-100-4, penetration as a function of particle size for three wind speeds.

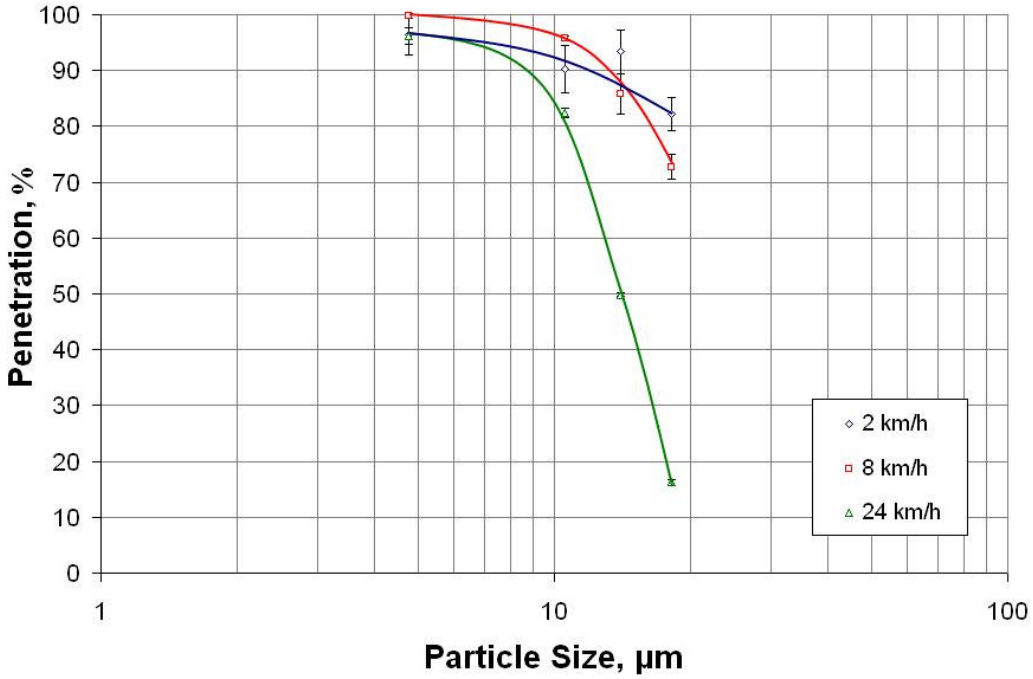

Figure 16: BSI-100-3, penetration as a function of particle size for three wind speeds.

Figure 17: BSI-100, penetration as a function of wind speed. Particle size: 10.1 µm AD.

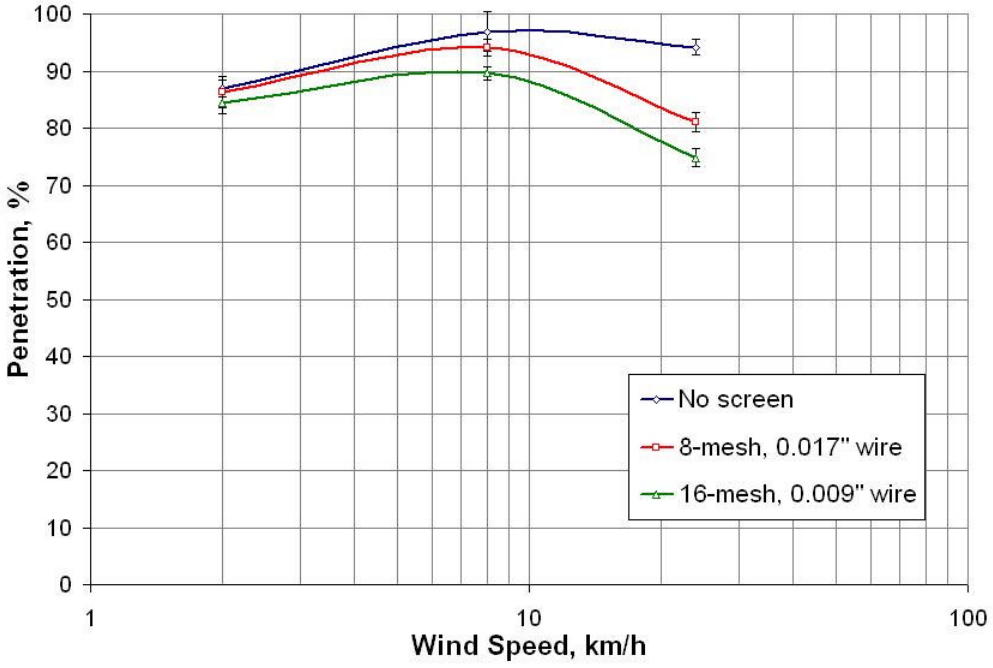

Figure 18: BSI-100, penetration as a function of wind speed for various screens. Particle size: 10.5 µm AD.

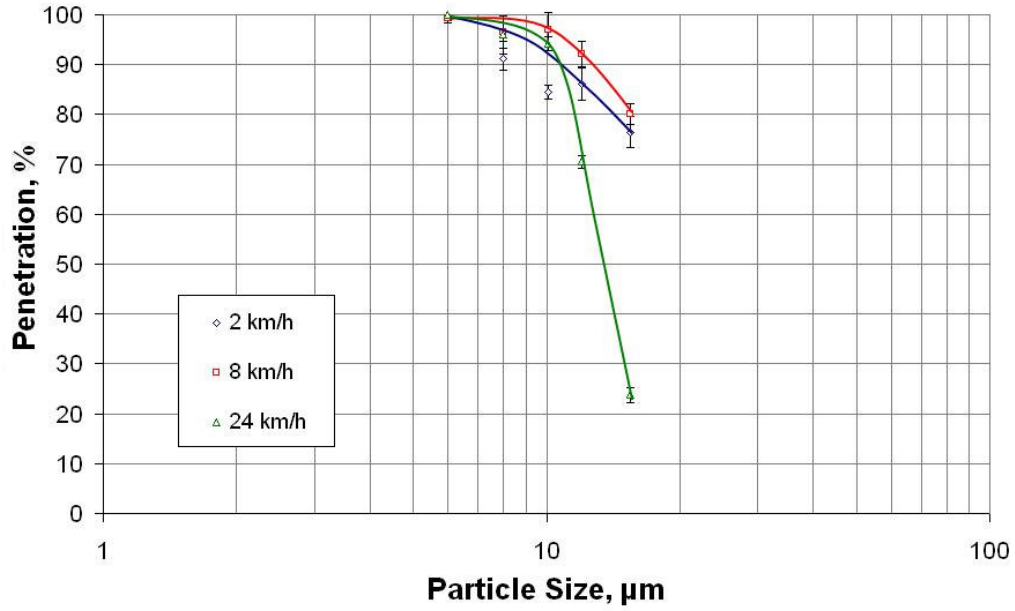

Figure 19: BSI-100, penetration as a function of particle size for three wind speeds.

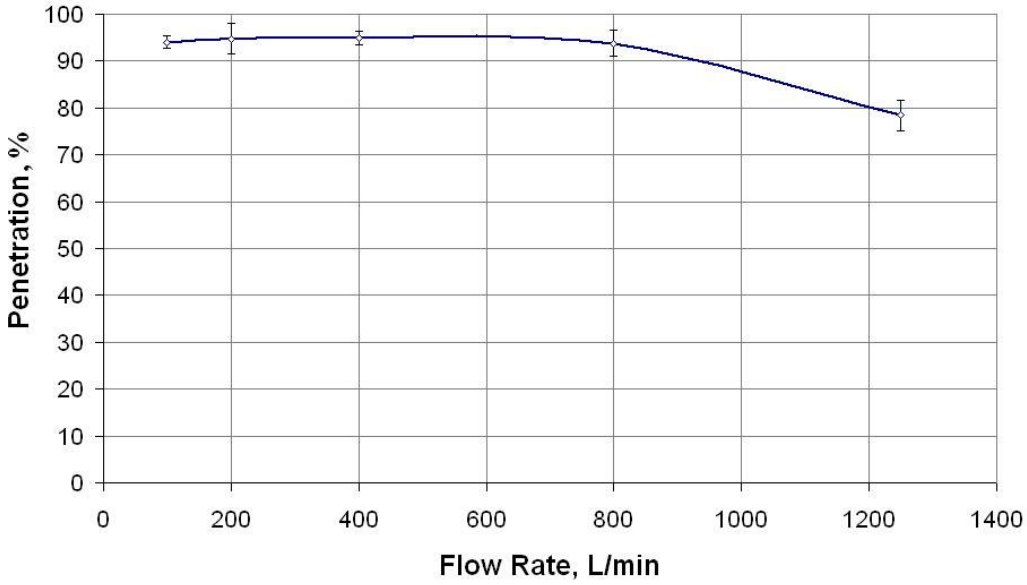

Figure 20: BSI-100, penetration as a function of operating flow rate at a wind speed of 8 km/h. Particle size: 10.4 to 10.7 µm AD.

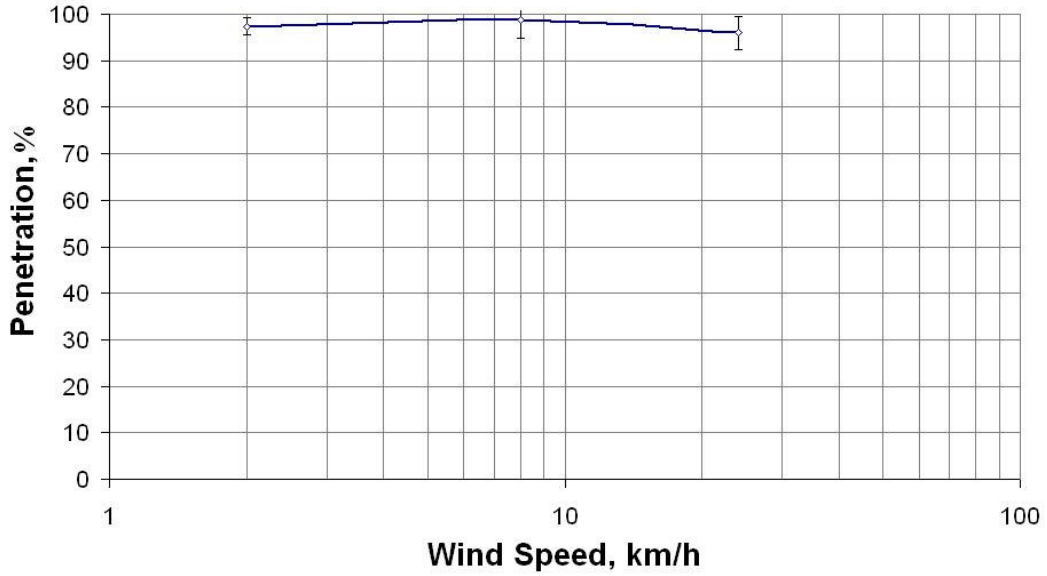

Figure 21: BSI-400, penetration as a function of wind speed. Particle size: 10.5 µm AD.

Figure 22: BSI-800, penetration as a function of wind speed. Particle size: 10.5 µm AD.

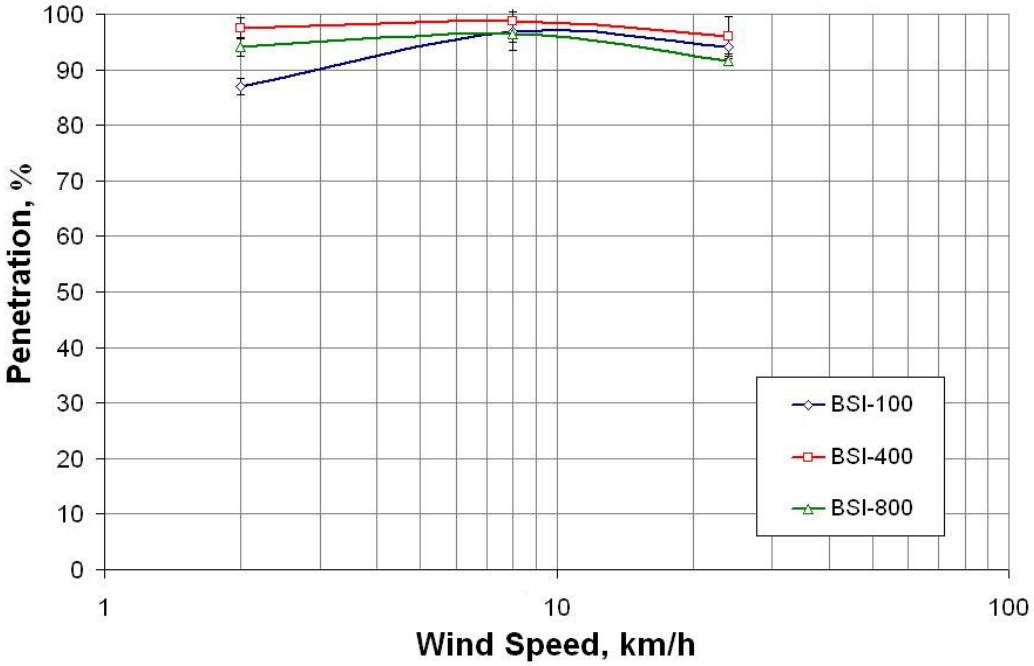

Figure 23: Penetration as a function of wind speed shown for all three BSI Units. Particle size: 10.5 µm AD.

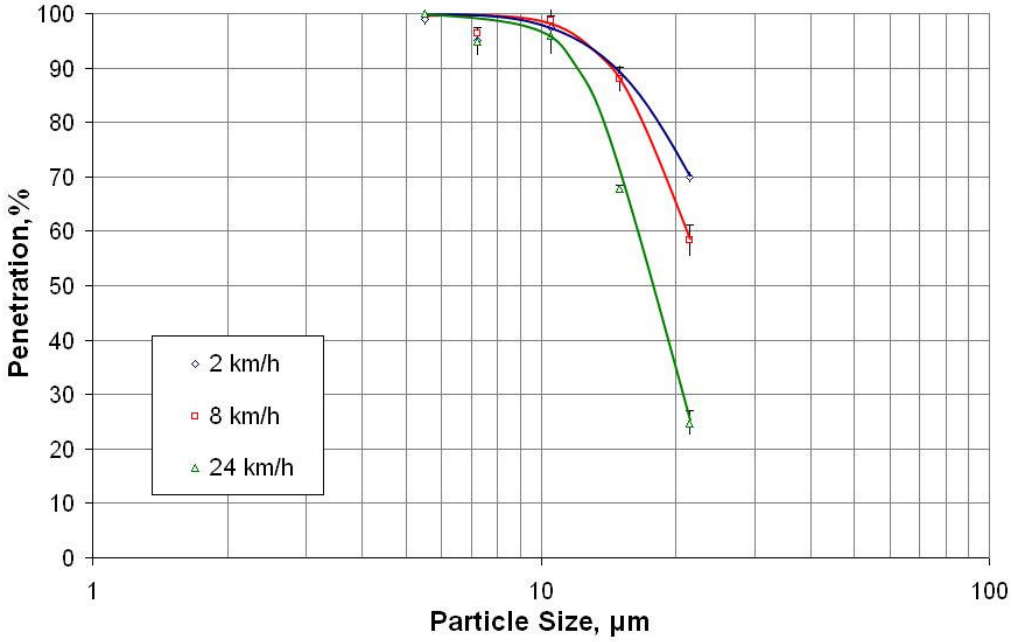

Figure 24: BSI-400, penetration as a function of particle size for three wind speeds.

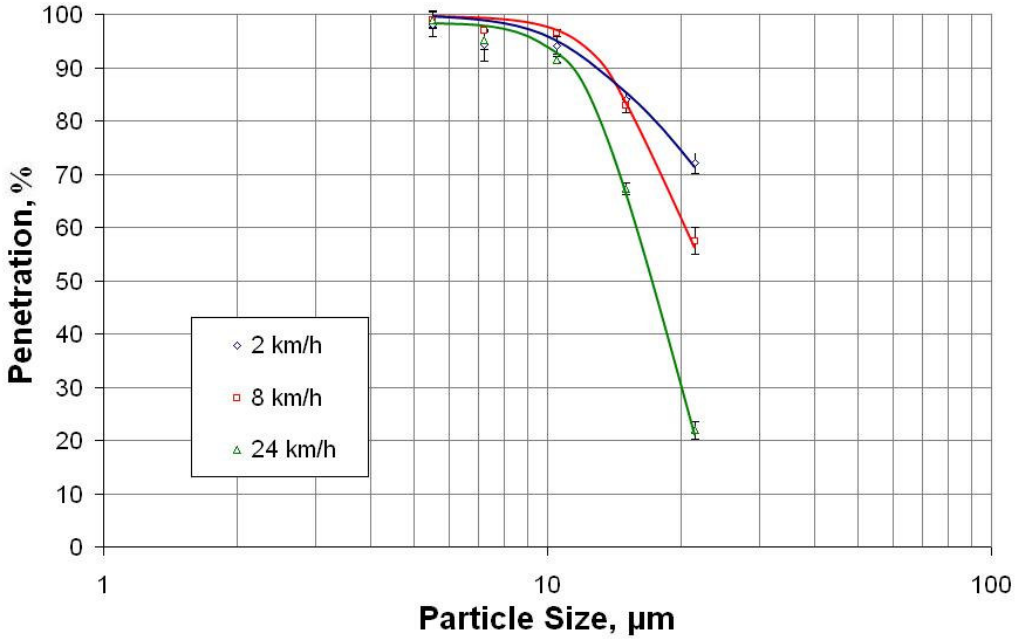

Figure 25: BSI-800, penetration as a function of particle size for three wind speeds.

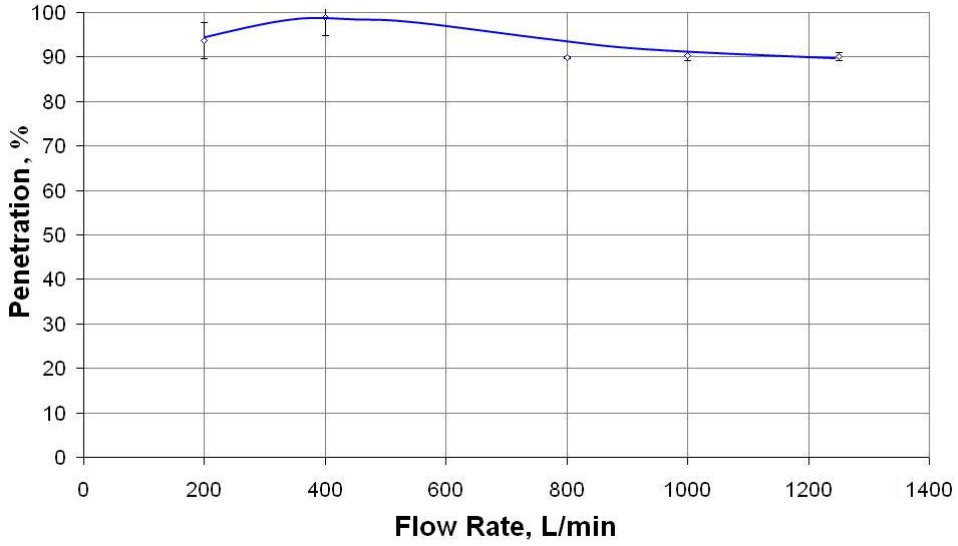

Figure 26: BSI-400, penetration as a function of flow rate at a wind speed of 8 km/h. Particle size: 10.5 µm AD.

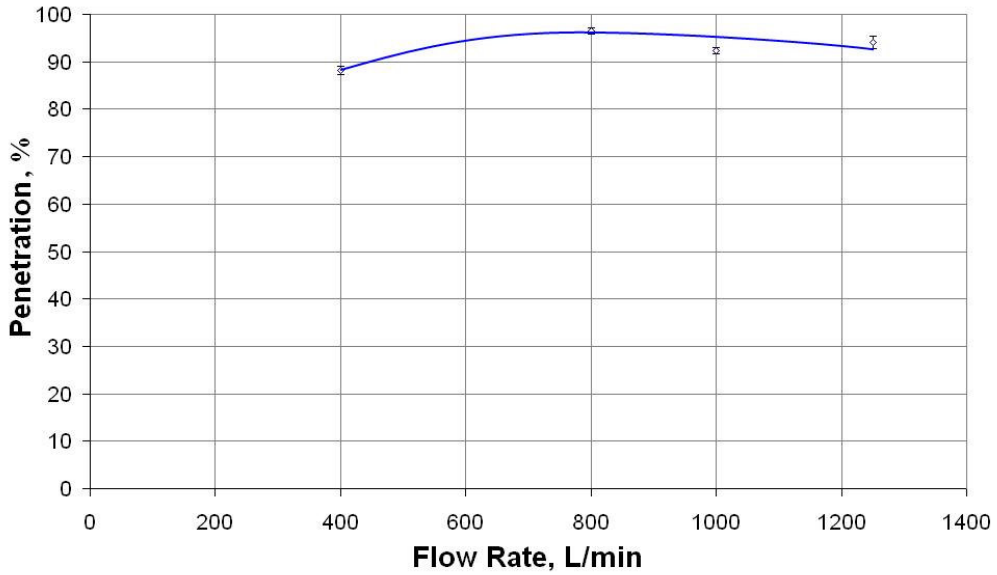

Figure 27: BSI-800, penetration as a function of flow rate at a wind speed of 8 km/h. Particle size: 10.5 µm AD.

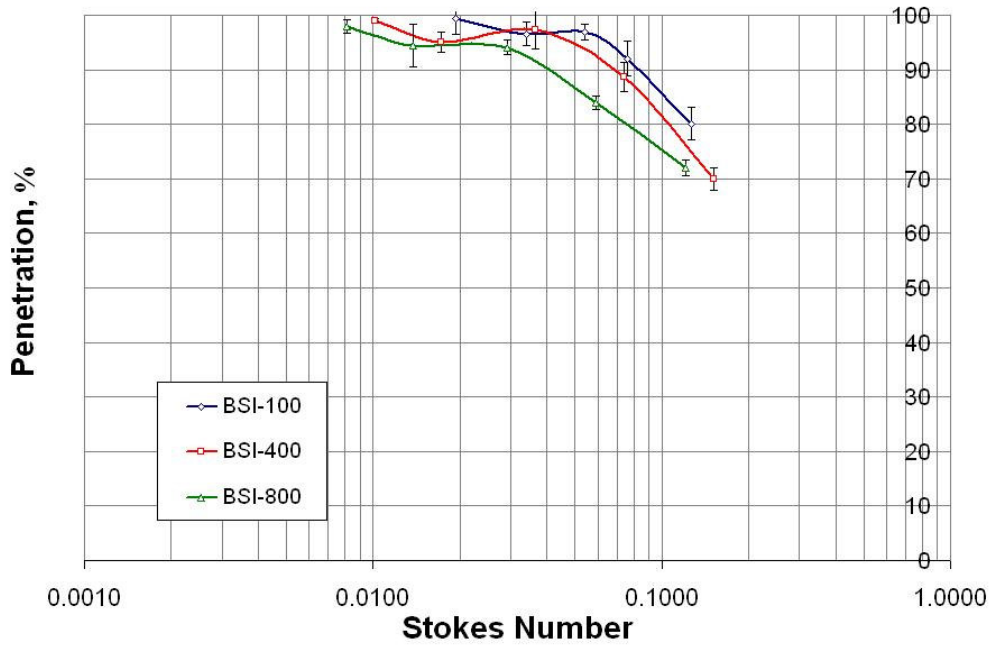

Figure 28: Penetration as a function of Stokes number at 2 km/h for all BSI inlets.

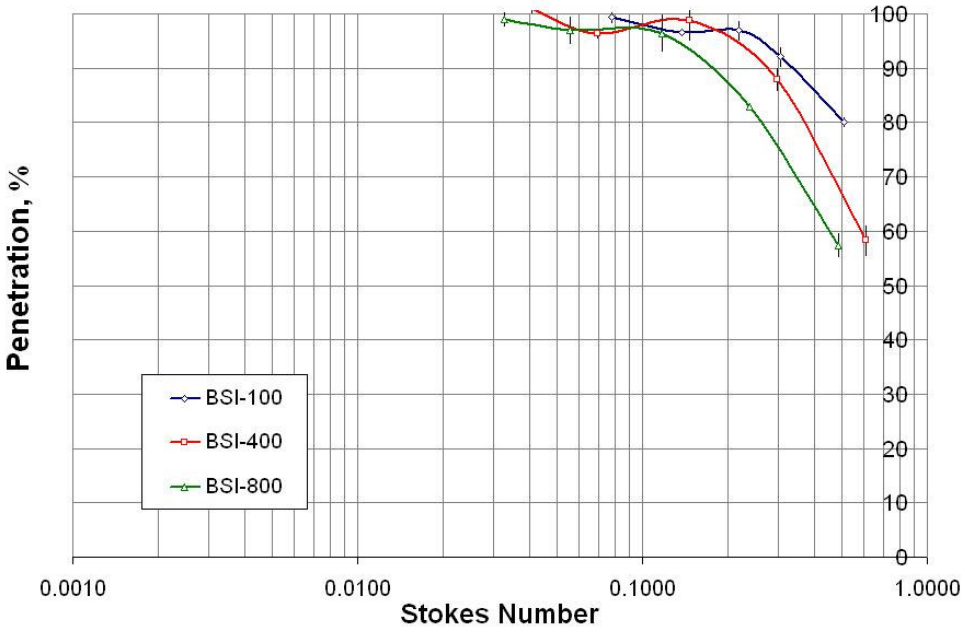

Figure 29: Penetration as a function of Stokes number at 8 km/h for all BSI inlets.

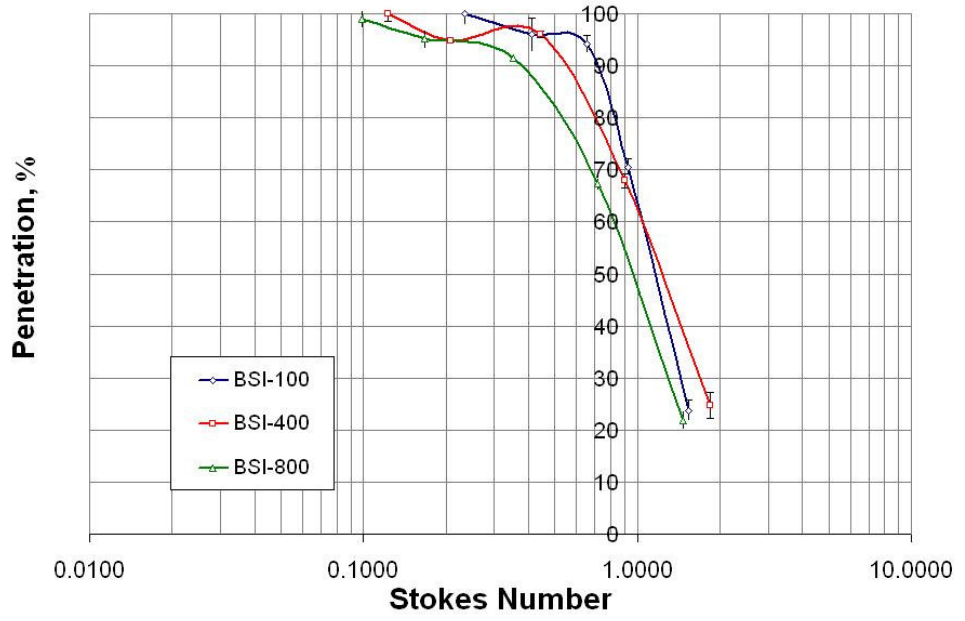

Figure 30: Penetration as a function of Stokes number at 24 km/h for all BSI inlets.

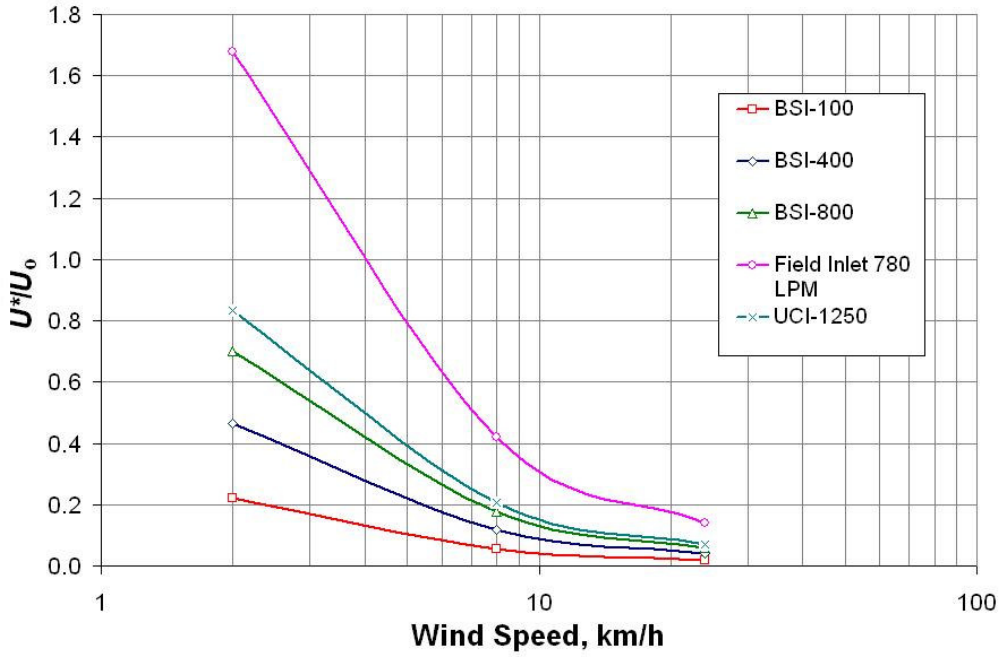

Figure 31: Modified velocity ratio as a function of wind speed for various omnidirectional inlets.

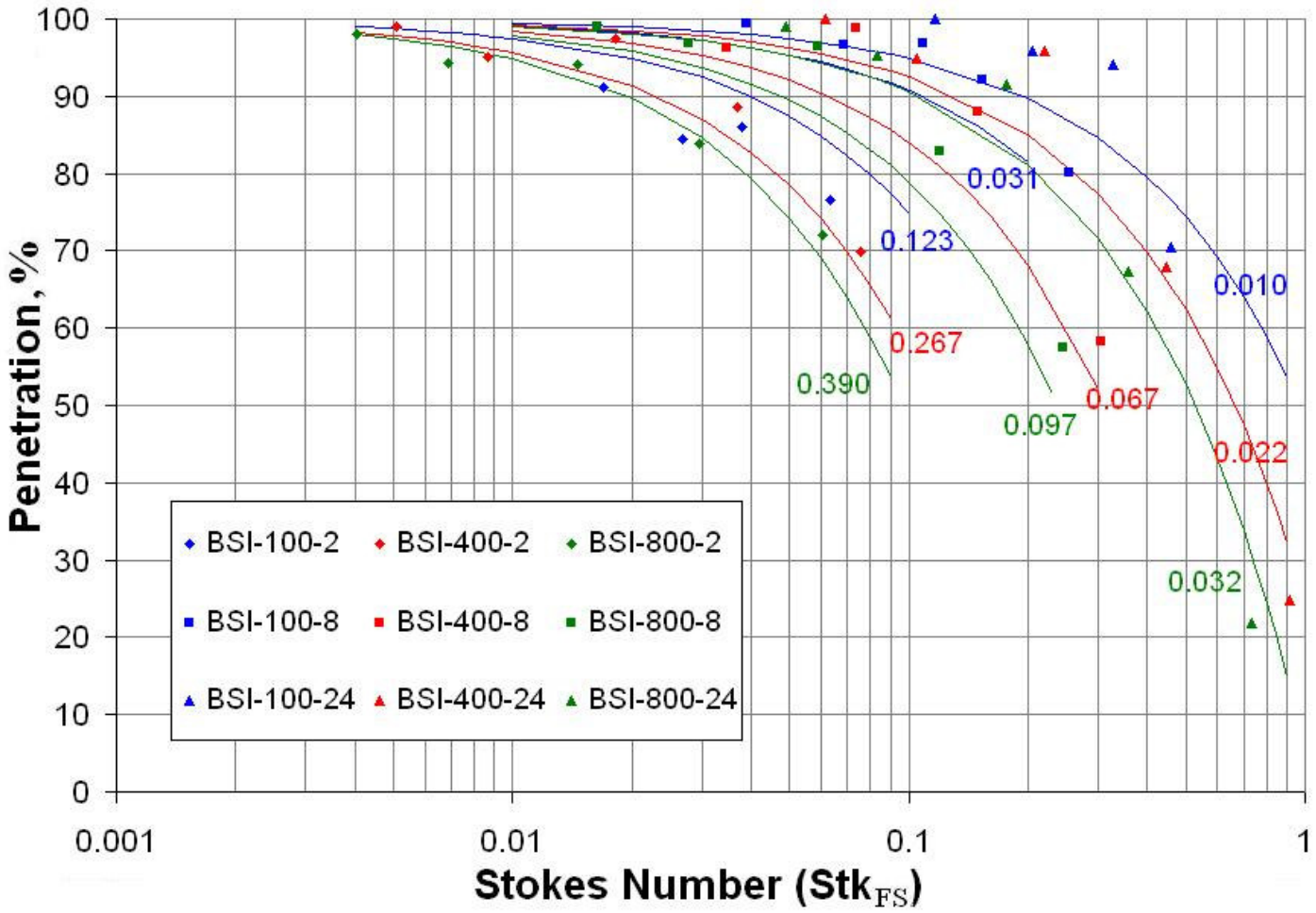

Figure 32: Penetration as a function of the Stokes number based on the free stream for various values of the modified velocity ratio. Scattered data points represent experimental results while the continuous curves are obtained from the correlation model representing the BSI inlet series.

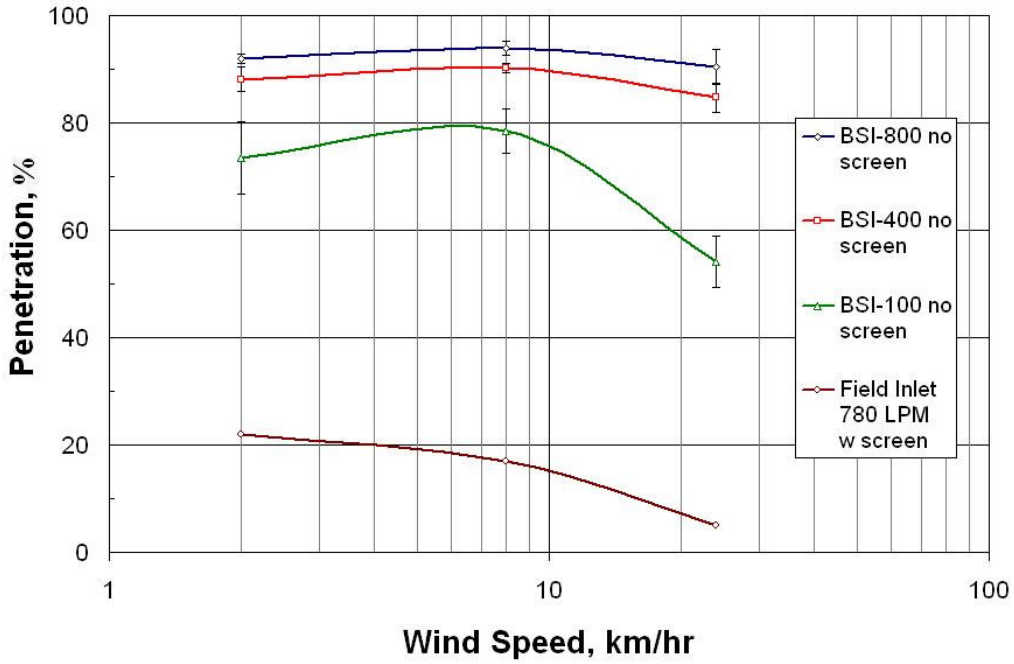

Figure 33: Comparison of the BSI series inlets operating at 1250 L/min with a currently deployed field inlet operating at 780 L/min. Particle size: 10.6 µm AD.

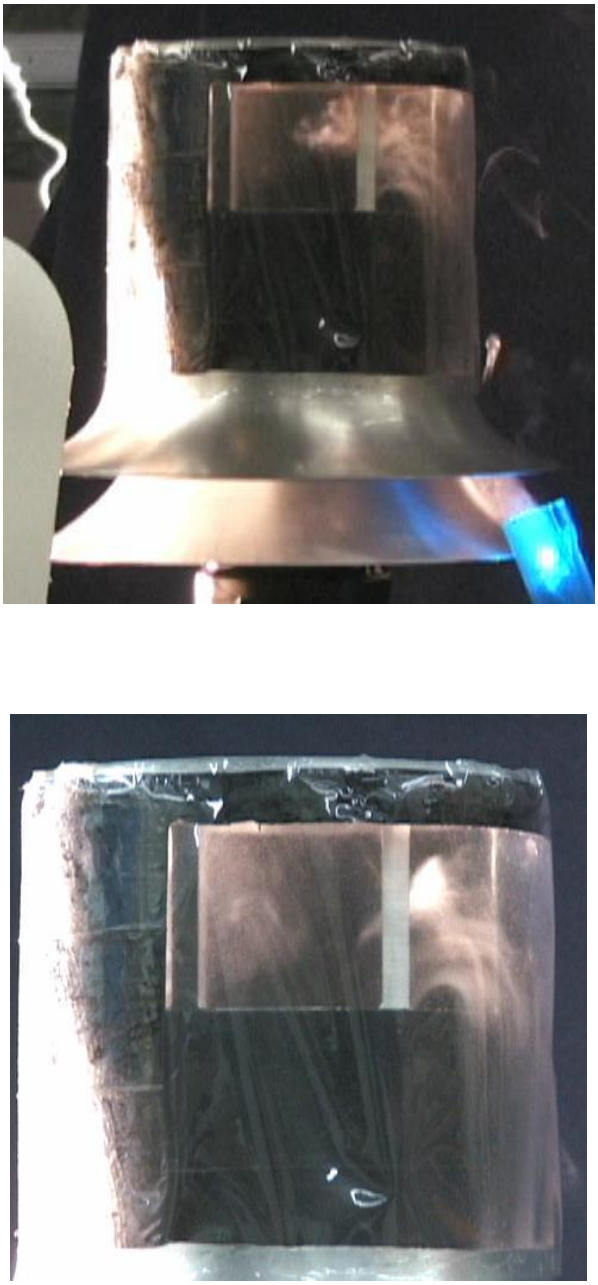

Figure 34: Flow visualization using smoke on the BSI-400 operating at 200 L/min.

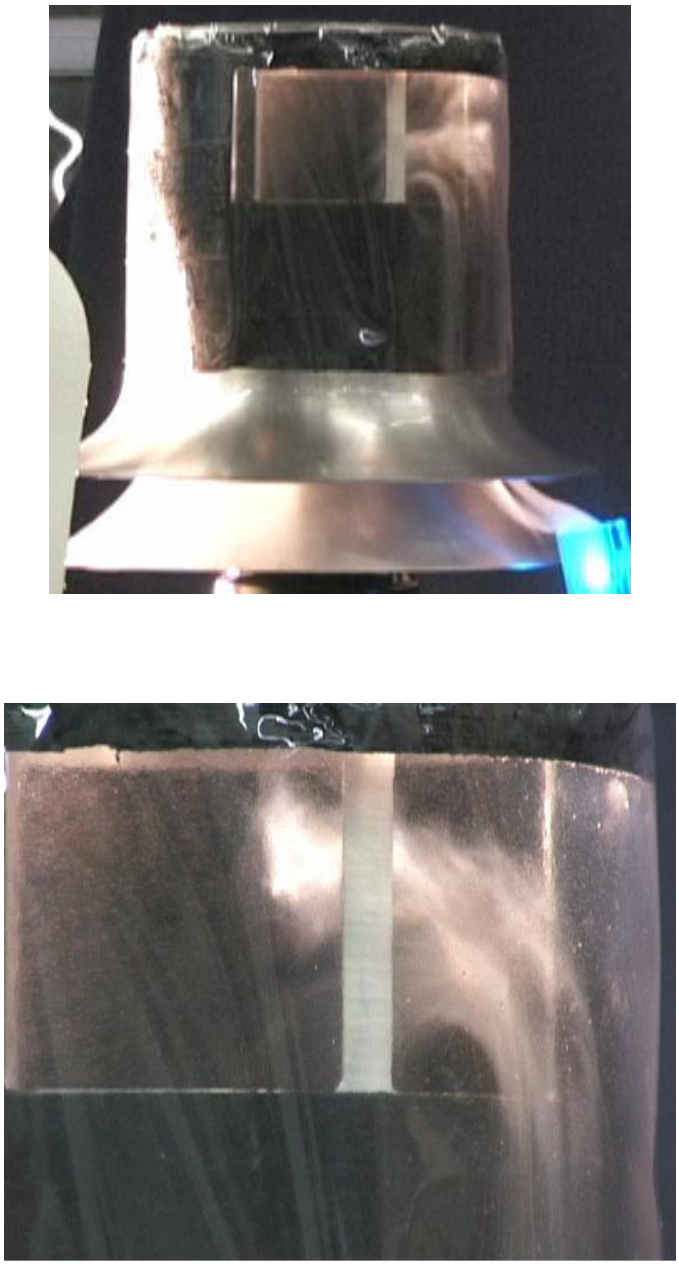

Figure 35: Flow visualization using smoke on the BSI-400 operating at 400 L/min.

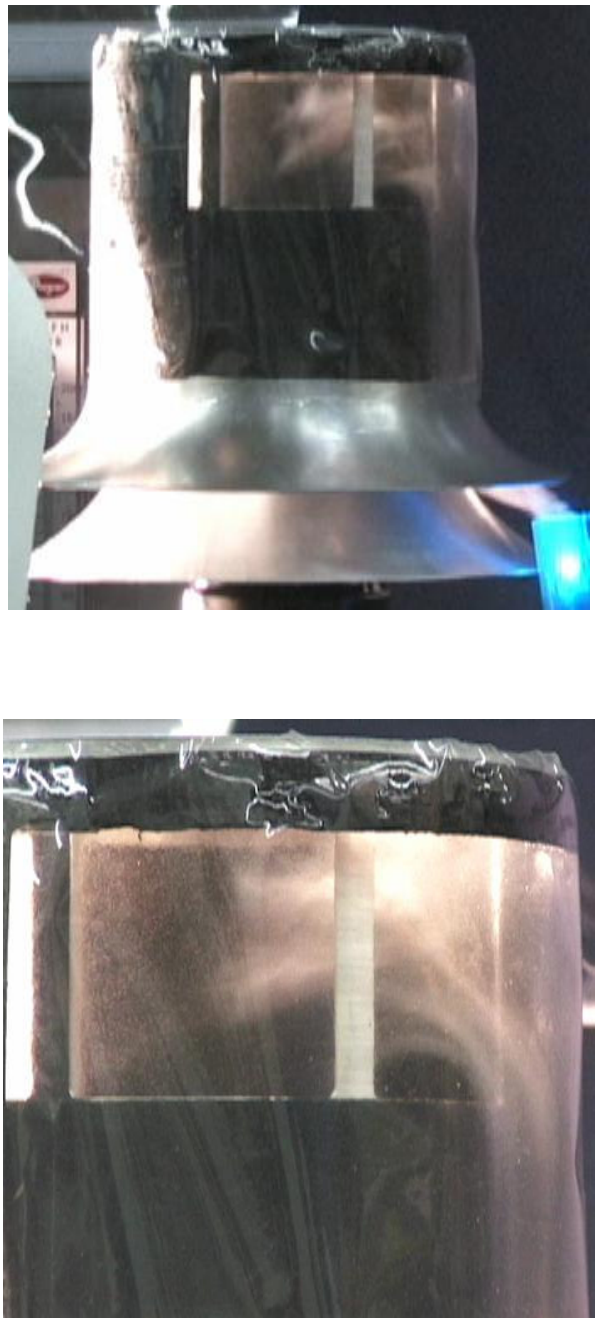

Figure 36: Flow visualization using smoke on the BSI-400 operating at 800 L/min.

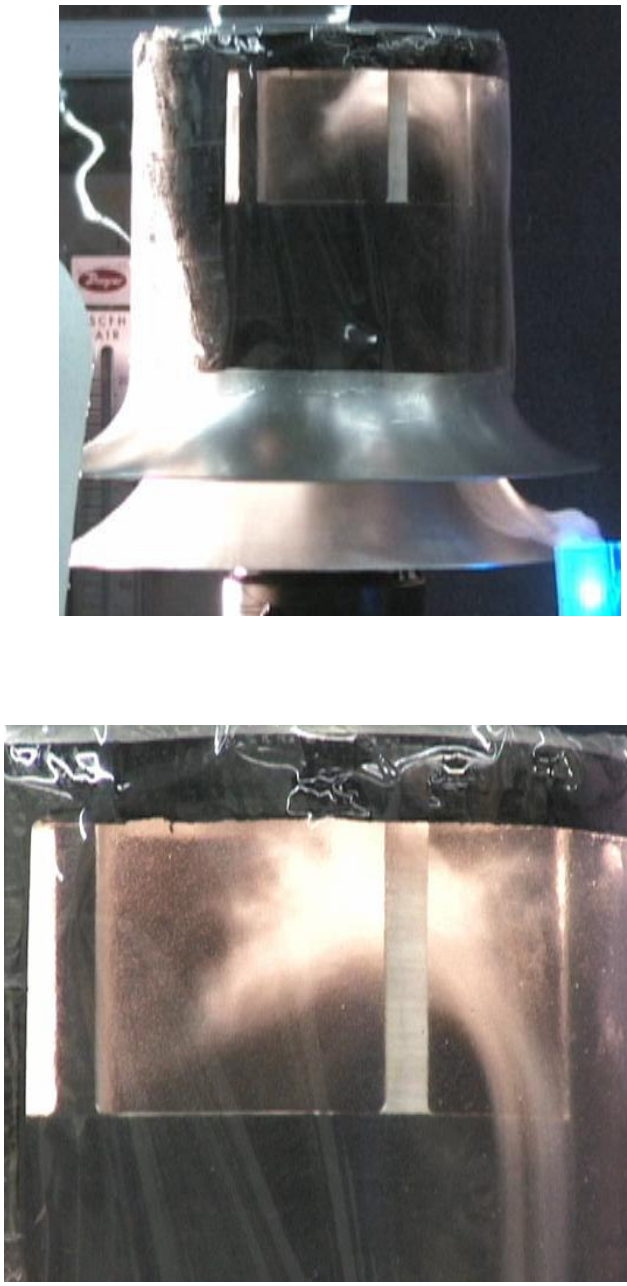

Figure 37: Flow visualization using smoke on the BSI-400 operating at 1250 L/min.

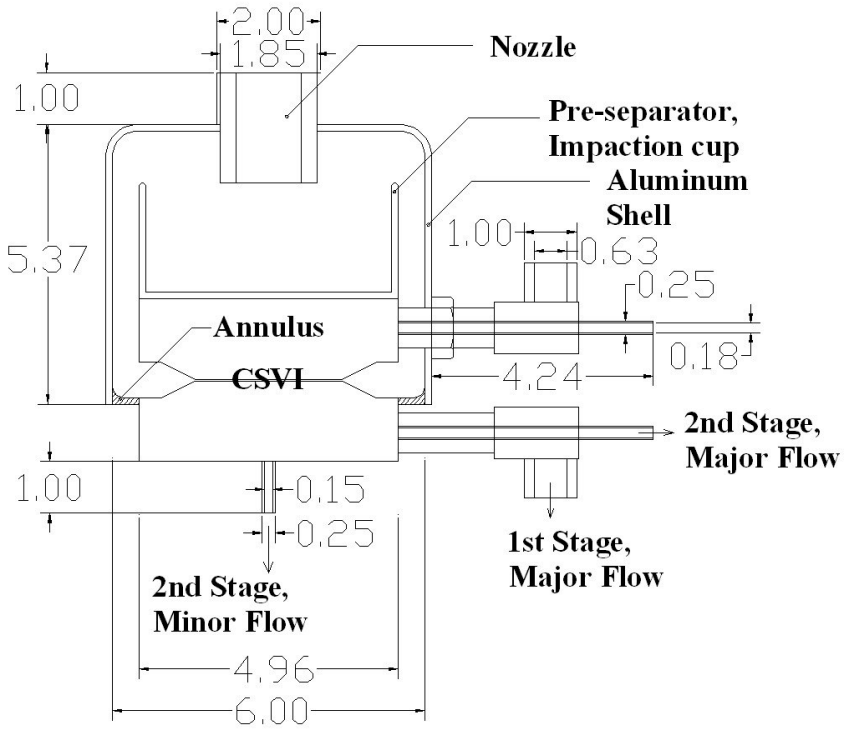

Figure 38: Schematic of the CSVI plenum and pre-separator assembly.

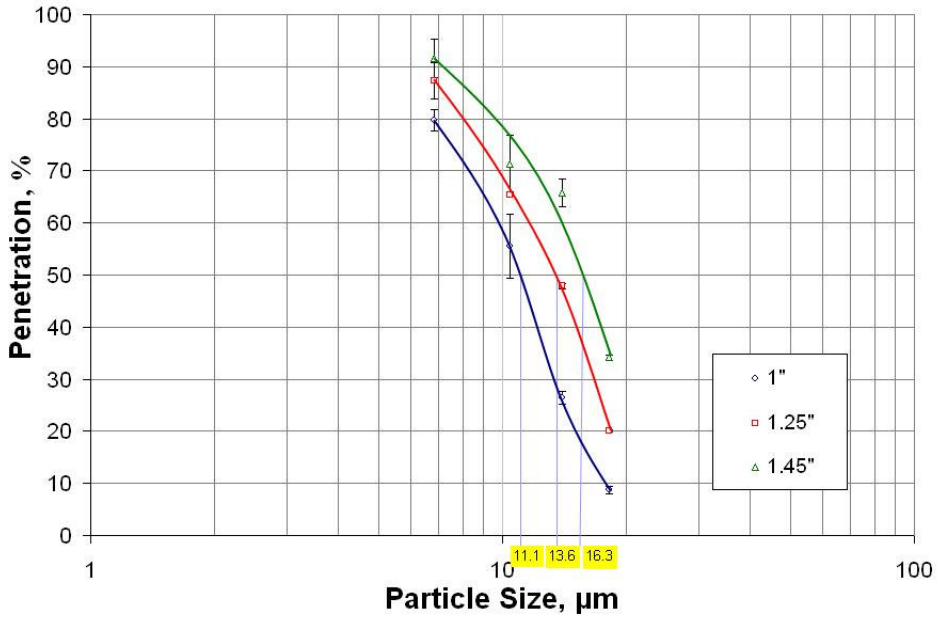

Figure 39: Penetration through the CSVI plenum as a function of particle size for three jet diameters.

VITA

Name: Rohit Ravindra Nene

Address: MS 3123, Department of Mechanical Engineering, Texas A&M University, College Station, TX 77843

Email Address: rohitnene@yahoo.com

Education: B. Tech., Mechanical Engineering, The Indian Institute of Technology, Madras, August 2003

M.S., Mechanical Engineering, Texas A&M University, May 2006